

Cite this: *Chem. Sci.*, 2023, 14, 3705

# Evolution and fabrication of carbon dot-based room temperature phosphorescence materials

Jiurong Li,<sup>a</sup> Yongzhong Wu<sup>b</sup> and Xiao Gong <sup>\*a</sup>

Traditional room temperature phosphorescence (RTP) materials usually include organometallic composites and pure organic compounds, which generally possess the disadvantages of high toxicity, high cost and complicated preparation. Carbon dots (CDs) are a new kind of luminescent material and have attracted widespread attention due to their benefits of excellent tunable emission, nice biocompatibility, cost-effectiveness, facile preparation and environmental friendliness. Since photoluminescence is an important luminescent property of carbon-based fluorescent nanomaterials, CD-based RTP materials have sparked a new research wave due to the properties of extremely long phosphorescence lifetime, large Stokes shift and high environmental sensitivity. In order to construct excellent CD-based RTP materials, many attempts have been made, and the corresponding progress has been achieved. Herein, we summarize the progress in CD-based RTP materials in recent years, mainly focusing on the outstanding contributions over the years, phosphorescence emission, phosphorescence lifetime, preparation and application of CD-based RTP materials. In particular, this review provides a comprehensive summary and analyze the outstanding contributions in the fields of the phosphorescence emission and phosphorescence lifetime of CD-based RTP materials over the years. Finally, several existing challenges and the future outlook of RTP materials based on CDs have been put forward.

Received 5th January 2023

Accepted 2nd March 2023

DOI: 10.1039/d3sc00062a

rsc.li/chemical-science

## 1. Introduction

Since the discovery of carbon dots (CDs) in 2004<sup>1</sup> and after nearly twenty years of development, researchers have put many efforts towards understanding them. As a new class of zero-dimensional fluorescent nanomaterials, CDs have attracted widespread concern and great research interest from a wide range of researchers owing to their distinguished properties such as adjustable photoluminescence (PL), excellent stability, facile surface functionalization, environmental friendliness, low toxicity and good biocompatibility.<sup>2–4</sup> According to previous reports,<sup>5</sup> CDs can be classified into four types, namely carbon nanodots (CNDs), carbon quantum dots (CQDs), graphene quantum dots (GQDs) and carbonized polymer dots (CPDs). Specifically, GQDs are small graphene fragments less than 20 nm in lateral dimension and less than five graphene flakes (~2.5 nm) in height, exhibiting pre-existing graphitic domains (sp<sup>2</sup> domains) and edge-rich chemical groups. CQDs are morphologically quasi-spherical carbon nanoparticles with a distinct lattice and chemical groups on their surface, and they have a crystalline core based on a mixture of sp<sup>2</sup> and sp<sup>3</sup>

domains. CNDs are also defined as quasi-spherical carbon nanoparticles, which consist mainly of cores with an amorphous structure, *i.e.*, CNDs have a certain degree of carbonization. CPDs have a hybrid polymer/carbon structure formed through the aggregation or cross-linking of linear polymers or monomers, with a surface consisting of abundant functional groups/polymer chains and carbon cores. Up to now, some notable achievements have been obtained in CD-related research, including the enhancement of photoluminescence quantum yield (PLQY), the regulation of multicolor fluorescence, the study of the luminescence mechanism and potential multifunctional applications.<sup>6–14</sup> More importantly, the selection of different carbon source precursors and synthesis methods will lead to different fluorescence properties. The fluorescence of CDs is only one of the most common phenomena in their luminescent properties. In addition, CDs also possess other types of excellent luminescent properties, such as room temperature phosphorescence (RTP), thermally activated delayed fluorescence (TADF), up-conversion luminescence (UCL), chemiluminescence (CL), electrochemical luminescence (ECL), mechanoluminescence and so on.<sup>15</sup> These luminescent properties have shown significant application prospects in biomedicine, optoelectronic devices, energy storage, sensing, anti-counterfeiting, catalysis, imaging and other fields.<sup>16–19</sup> Particularly, the RTP phenomenon of CDs has afterglow

<sup>a</sup>State Key Laboratory of Silicate Materials for Architectures, Wuhan University of Technology, Wuhan 430070, P. R. China. E-mail: xgong@whut.edu.cn

<sup>b</sup>School of Mechanical Engineering, Suzhou University of Science and Technology, Suzhou 215009, P. R. China

emission performance which is very attractive because of its prolonged emission lifetime, larger Stokes shift and minimized interference from short-lived auto-fluorescence and scattered light. Now it has shown a broad application prospect in anti-counterfeiting, information encryption, sensing and other advanced fields.

In the last twenty years, the research on CDs has been widely carried out, and people have also reviewed and summarized their fluorescence in various aspects, such as the classification, synthesis methods, fluorescence regulation, fluorescence mechanism, different precursor selection, and applications in various fields.<sup>6,8,10,14,20–34</sup> At the same time, the corresponding prospects for the fluorescence development of CDs are also proposed. Although there are some reviews providing a brief introduction of the afterglow phenomenon (*i.e.*, RTP and TADF) of CDs,<sup>15–19,35–38</sup> there are few articles specifically describing the afterglow phenomenon related performance in detail.<sup>39,40</sup> Based on the results previously reported, the radiative transition of triplet excitons is the key factor of the long afterglow phenomenon produced by CDs. The phosphorescence of CDs needs to be generated and enhanced by heteroatom doping or by embedding CDs into host matrices (*e.g.*, boric acid, polyvinyl alcohol, inorganic salts, layered double hydroxides, and zeolites) or by immobilizing CDs on a substrate. These matrices are essential for stabilizing the long-lived ternary state of CD fluorescence by effectively isolating and rigidifying CDs, minimizing the non-radiative leap of the triplet exciton and avoiding collisions of CDs with oxygen. In order to better distinguish the principal difference between fluorescence and phosphorescence, as shown in Fig. 1, the ground state ( $S_0$ ) transits to the lowest singlet excited state ( $S_1$ ) after being absorbed by ultraviolet and visible light, and then re-radiates back to  $S_0$  and emits fluorescence. The generated excitons first enter  $S_1$  from  $S_0$ , and then enter the lowest triplet state ( $T_1$ )

through the intersystem crossing (ISC) process, and the excitons return to  $S_0$  again and generate phosphorescence through the process of radiation transition. Or the exciton first goes through the process of reverse intersystem crossing (RISC), returns to  $S_1$  from  $T_1$ , and then returns to  $S_0$  to generate delayed fluorescence. Obviously, since the energy of  $T_1$  is lower than that of the singlet state  $S_1$ , the phosphorescent emission peak will be significantly red shifted compared with fluorescence. It is worth noting that the fluorescence phenomenon of CDs is easy to realize, but the RTP of CDs is much harder to achieve. This is mainly the result of the intrinsic properties of the triplet excitons in relation to the spin-forbidden transition. More importantly, the triplet exciton is readily exhausted by vibrational deactivation and oxygen quenching under room temperature or higher. Thus, it can be seen that in order to obtain effective RTP, two important conditions need to be met, namely to improve the rate of ISC by enhancing the spin-orbit coupling of excitons and to stabilize the triplet-excited states *via* using structural confinement. For the first condition, it is generally possible to enhance the n-p\* transition by incorporating transition metals, halogens or heterocycle groups to promote the ISC process and further generate triplet excitons. The second condition can be well achieved by encapsulating CDs in various substrates or creating self-protective structures (without substrate immobilization). Up to now, some efforts have been made to realize CD-based RTP materials to further explore their potential applications. Although some achievements have been made in the synthesis, construction and application of CD-based RTP materials, so far no article has systematically and completely summarized and analyzed them. And also, there have been several reviews on CD-based RTP materials in recent years, but they are only summarized and analyzed unilaterally for the synthesis, application or construction of CD-based RTP materials. Therefore, this review

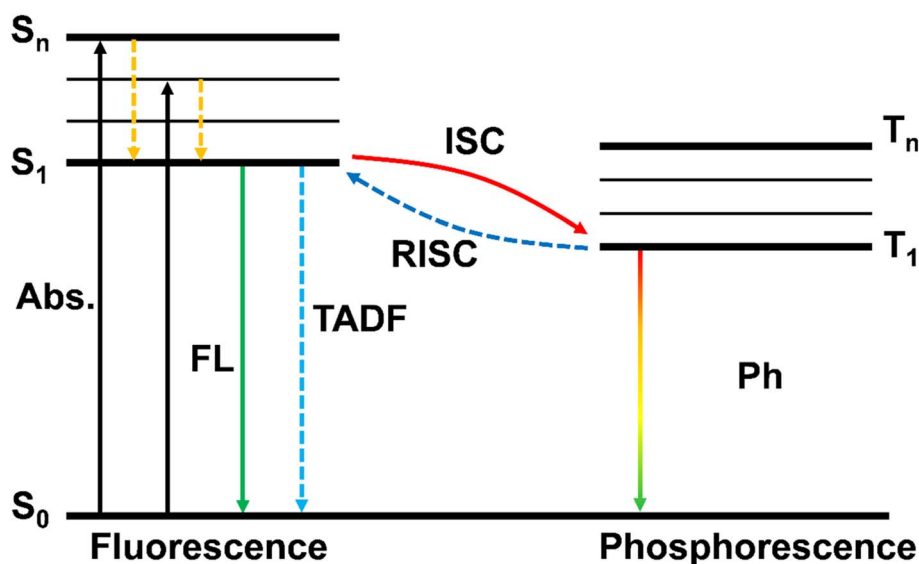


Fig. 1 Schematic illustration of the adsorption and emission processes of fluorescence (FL), phosphorescence (Ph), and delayed fluorescence (DF).



Table 1 Matrix-assisted CD-based RTP materials<sup>a</sup>

| Matrix  | Precursor   | Afterglow mode (298 K) | Afterglow emission (nm) | Afterglow lifetime ( $\tau$ ) ms <sup>-1</sup> (298 K) | PQY (%)  | Remarks  | Ref. |
|---|---|------------------------|-------------------------|--|----------|--|------|
| PVA   | CDs and PVA   | RTP                    | ~500                    | 380  | NA       | CDs-PVA  | 42   |
|   |   | RTP + TADF             | 569                     | 1610   | NA       | CDs/PVA  | 43   |
|   |   | RTP                    | 422                     | 338.4  | 6.88     | CDs-OH/PVA   | 44   |
|   |   | RTP + TADF             | 435                     | 567  | 6.24     | CNDs - PVA   | 45   |
|   |   |                        | 505                     | 1387   | 12.32    |  |      |
|   |   |                        | 560                     | 726  | 4.32     |  |      |
| KAl(SO <sub>4</sub> ) <sub>2</sub> ·x(H <sub>2</sub> O) | CDs and KAl(SO <sub>4</sub> ) <sub>2</sub> ·x(H <sub>2</sub> O) | RTP                    | 500                     | 655  | NA       | CD-KAl(SO <sub>4</sub> ) <sub>2</sub> ·x(H <sub>2</sub> O) | 46   |
|   |   |                        |                         |  |          | HN powder  |      |
|   |   |                        |                         |  |          |  |      |
| Urea  | CDs and urea  | RTP                    | 490                     | 1.06   | 7%       | NCD1-C   | 47   |
| Urea  | CDs and urea  | RTP + DF               | 500                     | 1020   | 7.23     | NCD2-C   | 48   |
|   |   |                        | 502                     | 1110   | 14.0     | NCD3-C   |      |
|   |   |                        | 625                     | 780  | 11.0     |  |      |
|   |   |                        |                         |  |          |  |      |
| PU  | N-doped CQDs and PU   | RTP + DF               | 500                     | 8.7  | NA       | CQD/PU   | 49   |
|   |   |                        | 525                     | 386.8  | 5.99     | CDs-LDHs   | 50   |
|   |   |                        | 490                     | 800  | 9.44     | Zn-CDs-LDH   | 51   |
|   |   |                        | 490                     | 719.9  | 9.58     | Zn-CDs-LDH   | 52   |
| SiO <sub>2</sub>  | m-CDs and colloidal nanosilica                                  | RTP + TADF             | 470                     | 703  | NA       | m-CDs@nSiO <sub>2</sub>                                    | 53   |
|   |   |                        |                         |  |          |  |      |
|   | CDs and silica nanoparticles                                    | RTP                    | 520                     | 1640   | NA       | CDs@SiO <sub>2</sub>                                       | 54   |
|   | CDs and nanosilica  | RTP + TADF             | 508                     | 1760   | NA       | CDs@SiO <sub>2</sub>                                       | 55   |
|   | CDs and silica  | RTP + TADF             | 507                     | 1620   | NA       | CDs@SiO <sub>2</sub>                                       | 56   |
|   | CDs and the SiO <sub>2</sub> matrix                             | RTP                    | 464                     | 5720   | 26.36    | CDs@SiO <sub>2</sub>                                       | 57   |
|   | CDs and silica  | RTP                    | 520                     | 1860   | 11.6     | WSP-CNDs@silica  | 58   |
|   | CNDs, Rhodamine B and silica                                    | RTP                    | 600                     | 910  | 3.56     | CNDs-RhB@silica  | 59   |
|   | CNDs and tetraethoxysilane                                      | RTP                    | 520                     | 1570   | 12.6     | CNDs@silica  | 60   |
|   | CDs, fluorescent dyes and amorphous silica                      | RTP                    | 510 to 610              | 1610 to 1260   | NA       | PCDs   | 61   |
|   | CDs and silica gel  | RTP                    | 525                     | 1800   | NA       | CDs in silica gel  | 62   |
| Zeolites  | CDs and a series of zeolites                                    | RTP + TADF             | 430                     | 350  | NA       | CDs@zeolite  | 63   |
|   |   |                        |                         |  |          |  |      |
|   | CDs and zeolite   | RTP                    | 500                     | 22.32  | 14.1     | CDs@zeolite  | 64   |
|   |   |                        | 620                     | 1.81   | 5.7      |  |      |
|   | CDs and zeolite   | RTP + TADF             | 525                     | 574  | NA       | CDs@zeolite  | 65   |
|   |   |                        | 440                     | 153  |          |  |      |
|   | CDs and zeolite   | RTP + TADF             | 530                     | 2100   | 24.4     | CDs@zeolite  | 66   |
|   | CDs, Eu <sup>3+</sup> and AlPO <sub>4</sub> -5 zeolite          | RTP + TADF             | 516                     | 1400   | NA       | CDs@EuAPO-5  | 67   |
| NaCl  | CDs and NaCl  | RTP                    | 516–520                 | 380–2100   | NA       | CDs@zeolite  | 68   |
|   |   |                        | 519                     | 314  | NA       | CD-NaCl  | 69   |
| Cyanuric acid   | CDs and cyanuric acid   | RTP                    | 480                     | 705  | 14       | CD-CA  | 70   |
|   |   |                        | 480                     | 687  | NA       | CD-CA  | 71   |
|   |   | RTP + TADF             | 550                     | 220.74   | NA       | CD@CA  | 72   |
|   |   |                        | 690                     | 13.29  |          |  |      |
|   |   |                        |                         |  |          |  |      |
| ZnAl <sub>2</sub> O <sub>4</sub>                        | CDs and urea  | RTP                    | 425–510                 | >2 hour  | NA       | m-CDs@CA   | 73   |
|   | CDs and cyanuric acid   | RTP                    | 416 and 550             | 1740   | 23.2     | m, p-CDs@CA  | 74   |
|   | CDs and zinc aluminate  | RTP                    | 517–650                 | NA   | NA       | CDs-ZnAl <sub>2</sub> O <sub>4</sub>                       | 75   |
|   | CDs and boric acid  | RTP                    | 490–570 nm              | 2.26   | 17.5     | a-CDs/BA   | 48   |
|   | CDs and boric acid  | RTP + TADF             | 454–500                 | 783  | NA       | GQD@BNO  | 76   |
|   | Lycorine hydrochloride and boric acid                           | RTP                    | 520                     | 1760   | 30       | CDs/BA   | 77   |
|   | CDs and boric acid  | RTP + TADF             | 475–555                 | 445.9  | 17.61    | CDs/B <sub>2</sub> O <sub>3</sub>                          | 78   |
| MOF   | CDs and boric acid  | RTP                    | 530                     | 1670   | 48       | g-t-CD@BA  | 79   |
|   | CDs and MOF   | RTP                    | 478–631                 | 85.67–1064.21  | 6.5–18.6 | CDs@MOF  | 80   |
|   | CDs and Mn-framework  | RTP                    | 530                     | 10.48  | NA       | CDs@MnAPO-CJ50   | 81   |
| Melamine  | CDs and melamine  | RTP                    | 620                     | 10.94  | 9.6      | CDs@MnAPO-tren   |      |
|   |   |                        | 529                     | 664  | 25       | M-CDs  | 82   |



Table 1 (Contd.)

| Matrix               | Precursor                 | Afterglow mode (298 K) | Afterglow emission (nm) | Afterglow lifetime ( $\tau$ ) ms <sup>-1</sup> (298 K) | PQY (%) | Remarks       | Ref. |
|----------------------|---------------------------|------------------------|-------------------------|--|---------|---------------|------|
| Clay                 | CDs and clay              | RTP + DF               | 450                     | 1050   | 6.06    | CDs@clay      | 83   |
|                      |                           |                        | 471                     | 1020   | 8.27    |               |      |
|                      |                           |                        | 530                     | 608  | 1.08    |               |      |
| Polyvinylpyrrolidone | CDs and PVP               | RTP                    | 580                     | 582  | NA      | CD/PVP        | 84   |
| Cellulose            | CDs and cellulose fibrils | RTP                    | 560                     | 167.31   | NA      | CDs@cellulose | 85   |

<sup>a</sup> NA: not available; PQY: phosphorescence quantum yield; TADF: thermally activated delayed fluorescence; RTP: room temperature phosphorescence; DF: delayed fluorescence; *m*PDs: *m*-phenylene diamine; MOF: metal-organic framework; PVA: polyvinyl alcohol; PVP: polyvinylpyrrolidone; PU: polyurethane.

provides a summary and analyzes comprehensively CD-based RTP materials, and systematically classifies and analyzes the relevant published academic papers. From the first discovery of CD-based RTP materials to the current research, it summarizes and analyzes some important research in each year, especially the phosphorescence life study of CD-based RTP materials.

## 2. Synthesis of CD-based RTP materials

Since the first report on CDs in 2004,<sup>1</sup> a variety of preparation methods have been reported successively, which can be mainly divided into two categories through summary analysis, namely, top-down approach and bottom-up approach.<sup>8,10,21,25–29,41</sup> As a special characteristic of CD-based luminescent materials, RTP has also been developed and reported. A variety of methods have also been reported for the synthesis of CD-based RTP materials, and they can also be mainly divided into two categories, namely matrix-assisted method (Table 1) and self-protection method (Table 2). The matrix-assisted method refers to the generation and enhancement of CD RTP by embedding them in a host matrix (*e.g.* boric acid, polyvinyl alcohol, layered double hydroxides, zeolites, *etc.*) or by immobilizing them on a substrate. This method has a wide range of practicality and can achieve the RTP properties of most CDs, but most of this method requires the use of multiple steps and harsh experimental conditions, often requiring high temperatures to achieve. The self-protection method means that the RTP properties of CDs are achieved by self-doping. This method is convenient, simple and highly scalable, but it is not suitable for large-scale preparation and it is difficult to find suitable precursors. At present, the most popular method is matrix-assisted synthesis. To date, in the preparation of metal free RTP materials, especially carbon-based RTP materials (mainly represented by CDs), more and more attention has been paid. The number of papers published is also increasing year by year, as shown in Fig. 2. As of August 31, 2022, a total of 166 articles related to CD-based RTP had been published through the keyword search of the paper. It is worth affirming that there may be omissions in the process of literature retrieval. We are sorry if some literature has not been retrieved.

### 2.1 Matrix-assisted synthesis of CD-based RTP materials

The matrix-assisted approach involves embedding CDs into appropriate matrix structures, such as polymeric matrices, crystalline structures, mesoporous structures, inorganic layer structures, *etc.* These matrices can provide a strong rigid environment, dense hydrogen bonding sites or strong covalent bonds that can lock their excited triplet states and suppress their non-radiative relaxation, resulting in RTP emission. To date, most CDs-based RTP has been achieved by embedding a number of matrices (Table 1), and many RTP CD-based matrix composites have been discovered by combining the outstanding PL properties of CDs with the effective confinement effects of various matrices.

Polymers are considered ideal matrices because of their rich functional groups and long regular chains, which not only provide stable chemical bonds with CDs, but also have the effect of separating solvent and oxygen and thus avoiding aggregation-induced fluorescence quenching. In particular, polyvinyl alcohol (PVA) was the first matrix material utilized to achieve CD-based RTP, which is currently the most commonly employed matrix support material.<sup>42–45,111–117</sup> In 2013, Deng *et al.*<sup>42</sup> first reported the observation of phosphorescence emission by compounding CDs with the PVA matrix (Fig. 3A). It is found that the PVA matrix plays a key role in protecting triplet states with long life from being effectively quenched by non-radiative processes, because it has a large number of hydrogen bonds that can effectively lock the emitting species and inhibit their intramolecular motions, *i.e.*, a non-radiative relaxation channel. In addition, PVA molecules also have a large number of hydroxyl groups, which can effectively form hydrogen bonds, making the C=O bond on the surface of CDs rigid, limiting the intramolecular motions and preventing non-radiative relaxation. Besides, oxygen is a strong quencher of the triplet state, but PVA has excellent oxygen barrier properties. Therefore, another potential function of PVA is to effectively prevent the direct collision between aromatic carbonyls and oxygen molecules, thereby promoting phosphorescence. Mesoporous materials are also a suitable class of matrix-assisted materials for achieving the RTP properties of CDs, which are a class of amorphous, ordered or crystalline materials with pore sizes of 2–50 nm that are good host matrices, and



Table 2 Self-protection CD-based RTP materials<sup>a</sup>

| Method                           | Precursor   | Afterglow mode (298 K) | Afterglow emission (nm)  | Afterglow lifetime ( $\tau$ ) ms <sup>-1</sup> (298 K) | PQY (%)                  | Remarks                     | Ref. |
|----------------------------------|---|------------------------|--------------------------|--|--------------------------|-----------------------------|------|
| Hydrothermal                     | Citric acid and ethylenediamine                                     | RTP                    | 440                      | 0.16   | NA                       | CDs                         | 86   |
| Hydrothermal                     | PVA and ethylene diamine  | RTP                    | 564                      | 13.4   | NA                       | NCD                         | 87   |
| Hydrothermal                     | Polyacid and diamine  | RTP                    | 494                      | 658.11   | NA                       | CDs                         | 88   |
| Microwave-assisted               | Ethanolamine and phosphoric acid                                    | RTP                    | 535                      | 1460   | NA                       | URTP CDs                    | 89   |
| Heat treatment                   | Laspactic acid and D-glucose  | RTP                    | 515                      | 747  | NA                       | NCDs                        | 90   |
| Solvothermal                     | Glucose and (C <sub>2</sub> H <sub>5</sub> ) <sub>3</sub> N·3HF     | RTP                    | 455                      | 1210   | 3.45                     | FNCDs                       | 91   |
| Microwave-assisted               | Triethanolamine and phosphoric acid                                 | RTP                    | 518                      | 820  | 15.85                    | P-CDs                       | 92   |
| Hydrothermal                     | Acrylamide, urea and citric acid                                    | RTP                    | 519                      | 459  | NA                       | NCDs                        | 93   |
| Heat treatment                   | Urea and phosphoric acid  | RTP                    | 495                      | 320  | 23                       | SW-CPDs                     | 94   |
| Hydrothermal                     | Isophthalic acid and ethylenediamine                                | RTP                    | 510                      | 769  | NA                       | N-CDs                       | 95   |
| Carbonization                    | Citric acid and 2,4,6-trihydrazinyl-1,3,5-triazine                  | RTP                    | 476                      | 66.4   | 4.7                      | C-dots                      | 96   |
| Hydrothermal                     | Citric acid (CA) and basic fuchsin                                  | RTP                    | 550                      | 51.9   | 28                       | N-CDs                       | 97   |
| Solvent-free pyrolysis treatment | Hydroxyurea   | RTP                    | 570                      | 175  | 13                       | FP-CDs                      | 98   |
| Solvothermal                     | 5,5'-Disulfanediylbis(2-nitrobenzoic acid)                          | RTP                    | 426/520                  | 1.1  | NA                       | HCDs                        | 99   |
| Solvothermal                     | Phenol, cytosine, resorcinol, and phloroglucinol                    | RTP                    | 500<br>505<br>520        | 65<br>127<br>218                                       | NA                       | F, O-codoped CDs            | 100  |
| Microwave-assisted               | Polyethylenimine and phosphoric acid                                | RTP                    | 515                      | 565.19   | NA                       | N-CDs                       | 101  |
| Solvothermal                     | Fructose and diethylenetriamine                                     | RTP                    | 500                      | 1140   | 8.3                      | FNCDs                       | 102  |
| Hydrothermal                     | Diethylenetriamine, phosphoric acid and boric acid                  | RTP                    | 509<br>535<br>567<br>603 | 481<br>511<br>437<br>426                               | 8.7<br>6.3<br>3.2<br>1.5 | CPDs                        | 103  |
| Hydrothermal                     | Levofloxacin  | RTP                    | 555<br>630               | 354<br>237   | 4.2                      | CD@paper                    | 104  |
| Solvothermal                     | Urea, HCl, citric acid, DMF   | RTP + DF               | 500<br>572               | 314<br>462   | 5.8                      | CD powder                   | 105  |
| One-step melting                 | Boric acid  | RTP                    | 512<br>495<br>560        | 1740   | 66.13                    | (NACA) <sub>0.01%</sub> /BA | 106  |
| Hydrothermal                     | Silica and hexamethyleneimine                                       | RTP + TADF             | 508                      | 451  | NA                       | CDs@SiO <sub>2</sub>        | 107  |
| Solvent-free catalytic assistant | <i>o</i> -Phenylenediamine and AlCl <sub>3</sub> ·6H <sub>2</sub> O | RTP                    | 554                      | 243.2  | 2.8                      | M-CDs                       | 108  |
| Pyrolysis                        | Citric acid and boric acid  | RTP                    | 466–638                  | 113.9–581.76   | 0.42–13.74               | B-CD                        | 109  |
| Microwave-assisted               | 1-[3-(Trimethoxy silyl) propyl]urea and phosphoric acid             | RTP                    | 480–560                  | 1000   | 59.41                    | CPDs                        | 110  |

<sup>a</sup> NA: not available; PQY: phosphorescence quantum yield; TADF: thermally activated delayed fluorescence; RTP: room temperature phosphorescence; DF: delayed fluorescence; PVA: polyvinyl alcohol.

capable of accommodating luminescent species. As such, it is capable of accommodating CDs to achieve RTP, particularly silica, and is widely applied for the generation of CD RTP.<sup>53–60,107,118</sup> For example, Li *et al.*<sup>54</sup> proposed a strategy for achieving ultra-long RTP in air-saturated aqueous media based on carbon dot-based silica composites (CDs@SiO<sub>2</sub>) (Fig. 3B). The formation of Si–O–C bonds between CDs and silica during TEOS hydrolysis acts as a scaffold for the nucleation and the growth of the silica framework. The CDs are able to covalently attach to the silica network and the silica acts as a matrix that

contributes to the dispersion of the CDs, providing protection from environmental bursts such as water and oxygen. More importantly, the abundance of silanol groups on the surface of the composites gives the whole hybridized system a good hydrophilic character. And also, Sun *et al.*<sup>57</sup> designed and developed a strategy to fabricate metal-free multi-confined CDs (CDs@SiO<sub>2</sub>) within SiO<sub>2</sub> by generating an effective multi-confinement effect (MCE) to develop room temperature phosphorescent materials with simultaneous ultra-long lifetime, high phosphorescence quantum efficiency and







Fig. 2 The number of articles related to CD-based RTP since 2013; search results were obtained from the Web of Science, on 31st August 2022.

excellent stability (Fig. 3C). In addition, zeolites are a class of matrix-assisted materials widely utilized to achieve ultra-long phosphorescence lifetimes, and they are crystalline

aluminosilicates or aluminophosphates with a three-dimensional 4-connected structure and a uniform pore size of less than 2 nm.<sup>63–68,119</sup> For instance, Wang *et al.*<sup>64</sup> have achieved a facile strategy to modulate the RTP properties of CDs through donor–acceptor energy transfer in the CDs–zeolite system by introducing heteroatoms into the aluminium phosphate zeolite backbone to construct an efficient donor–acceptor system that promotes exchange coupling between the CD exciton and the dopant in the matrix (Fig. 3D). Furthermore, the confinement effect of the crystal structure not only immobilizes  $T_1$  but also prevents non-radiative relaxation of  $T_1$  and is also a promising method for generating CD-based RTP. Crystal structures can be divided into two categories: organic crystal structures and inorganic crystal structures. The organic crystal structures include urea, cyanuric acid and melamine, while inorganic crystal structures include sodium chloride, sodium hydroxide, boric acid and so on.<sup>46–48,70,72–76,78,79,82,120–130</sup> For example, Wang *et al.*<sup>124</sup> proposed a molten salt method for the preparation of CD-based RTP materials by selecting high charge density magnesium salts and phosphates as doping salts, and calcining the carbon source directly in the presence of inorganic salts (Fig. 3E). During the melting and recrystallization process, CDs are formed and incorporated into a matrix with a special crystal structure. As magnesium phosphate is insoluble in water, the solid matrix provides rigid protection for the CDs. As a result, the CDs are non-phosphorescent as monomers, but the RTP

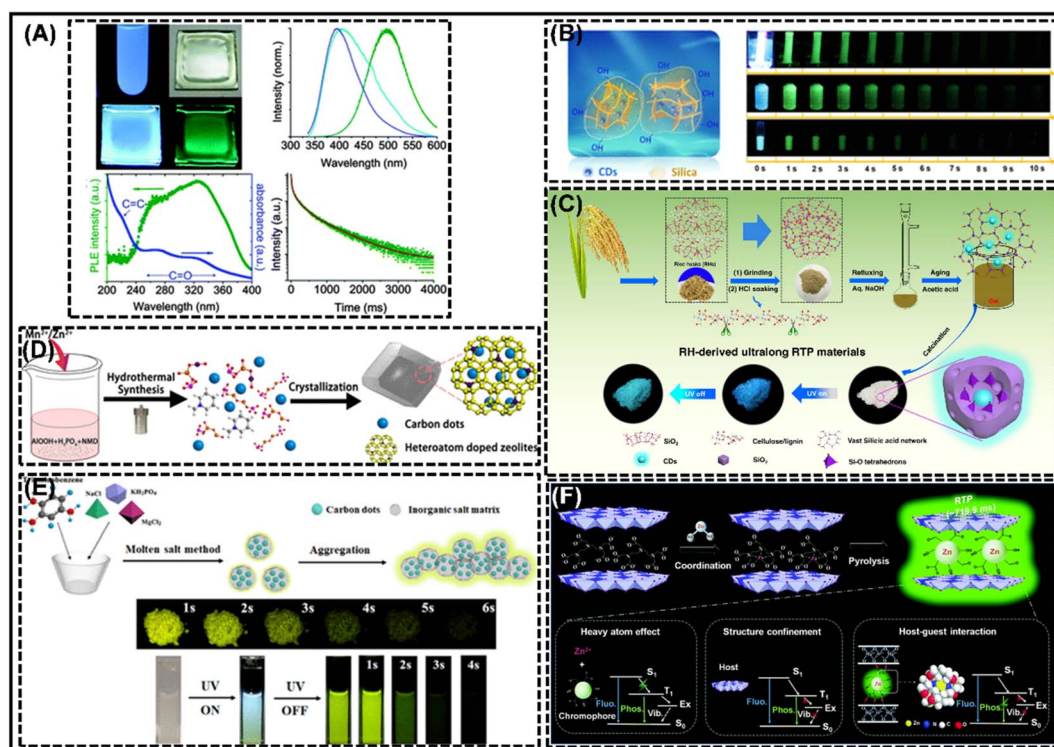


Fig. 3 Matrix-assisted synthesis of CD-based RTP materials. (A) Reprinted with permission from Deng *et al.*<sup>42</sup> Copyright 2013, Royal Society of Chemistry. (B) Reprinted with permission from Li *et al.*<sup>54</sup> Copyright 2019, American Chemical Society. (C) Reprinted with permission from Sun *et al.*<sup>57</sup> Copyright 2019, Springer. (D) Reprinted with permission from Wang *et al.*<sup>64</sup> Copyright 2019, American Chemical Society. (E) Reprinted with permission from Wang *et al.*<sup>124</sup> Copyright 2019, American Chemical Society. (F) Reprinted with permission from Kong *et al.*<sup>52</sup> Copyright 2019, Royal Society of Chemistry.

phenomenon is initiated and enhanced by the aggregation of the salt matrix. Besides this, structural confinement displays a unique advantage by reducing the rate of the radiative relaxation process. A number of special structural matrices have also been used for the realization of CD RTP, such as two-dimensional (2D) layered double hydroxides (LDHs) which have attracted significant interest in the available confinement matrix owing to their versatile chemical composition and layer charge. Significantly, LDHs have a nanoscale space that provides a constrained and rigid environment for a number of chromophores that exhibit enhanced fluorescence properties (intensity, efficiency, lifetime, *etc.*) by suppressing the non-radiative relaxation of single-linear excitons.<sup>52</sup> Therefore, exploring the relationship between the relaxation paths of triplet-state excitons and the rigidity of LDHs will help to achieve optimal luminescence efficiency and to develop a new class of RTP materials. Kong *et al.*<sup>52</sup> employed LDHs as a matrix and proposed the design principle of activation to achieve RTP on CDs through three synergistic effects (structure-bound effect, heavy atom effect, and chemical bonding) (Fig. 3F). The confined and rigid environment of LDHs suppressed the non-radiative deactivation of CD triplet excitons and improved the luminescence efficiency. In conclusion, in addition to the above matrix-assisted materials, there are also other appropriate matrix-assisted materials suitable for achieving RTP of CDs. Therefore, the appropriate selection of matrices is key to achieving efficient and ultra-long RTP CDs.

## 2.2 Self-protection synthesis of CD-based RTP materials

Although the RTP of CDs in solid and water-disperse states has been achieved, the CD-based RTP materials prepared by matrix-assisted methods are mostly heterogeneous systems with poor thermal stability and electrical conductivity, which hinders their practical application. Therefore, to overcome these issues, the development of matrix-free self-protected phosphorescent CDs is an urgent problem to be solved. Aiming to generate self-protected RTP of CDs, the choice of the raw material is crucial. Currently, researchers often choose polymers or their monomers, cross-linkable reactants, molecules doped with heteroatoms and larger conjugated structures as precursors.<sup>86–96,98–109,131,132</sup> The relevant achievements are shown in Table 2.

The earliest use of self-protection methods to achieve the RTP of CDs dates back to 2014, when Yan *et al.*<sup>86</sup> employed citric acid and ethylenediamine as carbon and dopant sources to achieve the RTP of CDs, but the phosphorescence lifetime at that time was only 160 ms, and thus this result did not attract widespread attention. Until 2016, Chen *et al.*<sup>87</sup> achieved the RTP of CDs in one step using PVA and ethylenediamine as reaction precursors, with a phosphorescence lifetime of up to 13.4 ms. At this time, the RTP of CDs gradually came into the limelight, and the research frenzy gradually surged. Later, Jiang *et al.*<sup>131</sup> by simple heat treatment of ethylenediamine and phosphoric acid could produce unexpectedly long room temperature

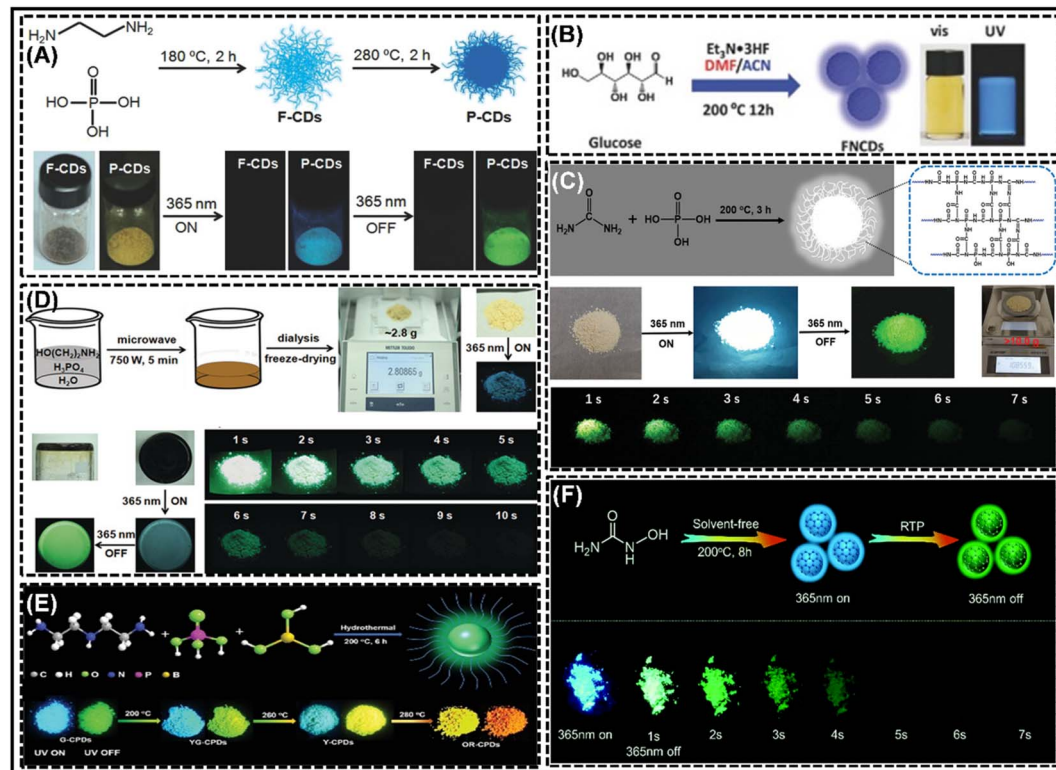


Fig. 4 Self-protection synthesis of CD-based RTP materials. (A) Reprinted with permission from Jiang *et al.*<sup>131</sup> Copyright 2018, Wiley-VCH. (B) Reprinted with permission from Long *et al.*<sup>91</sup> Copyright 2018, Wiley-VCH. (C) Reprinted with permission from Wang *et al.*<sup>94</sup> Copyright 2020, Wiley-VCH. (D) Reprinted with permission from Jiang *et al.*<sup>89</sup> Copyright 2018, Wiley-VCH. (E) Reprinted with permission from Wang *et al.*<sup>103</sup> Copyright 2021, Wiley-VCH. (F) Reprinted with permission from Zhao *et al.*<sup>98</sup> Copyright 2021, Royal Society of Chemistry.

phosphorescence with a duration of about 10 s and a lifetime of 1.39 s (Fig. 4A). It is suggested that the doping of N and P elements is the primary factor in achieving the RTP of CDs. And then, Long *et al.*<sup>91</sup> reported a new type of fluorine–nitrogen co-doped CDs, which were obtained by a one-step solvent heat treatment, exhibiting excellent water solubility and blue fluorescence in solution or on filter paper, together with pH-responsive green self-protective RTP (Fig. 4B). The spatial protection of C–F bonds and hydrogen bonds was found to reduce the quenching of RTP by oxygen at room temperature, which is key to achieving RTP in CDs. In addition, Wang *et al.*<sup>94</sup> have successfully engineered a one-step approach for the synthesis of gram-scale CDs with up to 41% total QY by utilizing the polymerization, deamination and dehydration reactions of urea and phosphoric acid in an aqueous environment (Fig. 4C). It was similarly demonstrated that doping with N and P was responsible for achieving white light emission. Also, Jiang *et al.*<sup>89</sup> reported a facile, rapid, gram-scale preparation of ultra-long RTP CDs by employing microwave-assisted heating of aqueous solutions of ethanolamine and phosphoric acid (Fig. 4D). Further studies showed that the amorphous polymer-like structure of the CDs, intraparticle hydrogen bonding and the presence of doping elements N and P were the major factors responsible for their ultra-long RTP. Furthermore, Wang *et al.*<sup>103</sup> proposed a thermally driven amorphous-crystalline phase transition-based strategy to achieve multicolor CPDs with emission colors adjustable from green to orange-red. Further studies have shown that self-protected covalent crosslinking framework formation as well as the co-doping of multiple heteroatoms play a crucial role in the generation of RTP CDs. The color tunability of RTPs can be attributed to the different crystalline contents of conjugated  $\pi$ -domains within the CPDs (Fig. 4E). Similarly, Zhao *et al.*<sup>98</sup> demonstrated that efficient blue-green fluorescent-phosphorescent double-emitting CDs could be easily obtained *via* solvent-free pyrolysis of hydroxyurea (Fig. 4F), and it was demonstrated that the efficient double-emitting properties of the fluorescent-phosphorescent CDs were derived from the aromatic carbonyl group at their edges. In summary, co-doping (e.g. N and P co-doping or N and F co-doping) strategies are one of the most effective means applied to achieve ultra-long and efficient synthesis of RTPs with self-protected CDs. In addition, the rational use of edge groups (carbonyl groups) is also expected to achieve self-protected RTP CDs.

### 3. Annual representative studies on CD-based RTP materials

According to the synthetic methods described earlier, the synthesis of CDs RTP has been a positive achievement, with progress being made every year. In each year of work, different matrices or methodologies have been employed to fabricate high performance RTP CDs, and the corresponding structures of the resulting RTP CDs varied. Examples include the use of doping to form covalent bonds to achieve RTP of CDs by self-protection<sup>91</sup> (Fig. 5A), the use of cyanuric acid<sup>74</sup> (Fig. 5B) and

boric acid<sup>77</sup> (Fig. 5C) as substrate-assisted methods to form rigid structures to encapsulate immobilized CDs to achieve RTP, the use of silica<sup>55</sup> (Fig. 5D) and zeolites<sup>63</sup> (Fig. 5E) as mesoporous media materials to encapsulate immobilized CDs to achieve RTP, and the use of layered double hydroxides<sup>51</sup> (Fig. 5F) as media to immobilize CDs by intercalation to achieve RTP. So far, some significant achievements about RTP CDs have been realized and are shown in Fig. 5G. All these studies were outstanding contributions and prominent representatives in that year, but they were not ranked in the same year. In 2013, Deng *et al.*<sup>42</sup> employed PVA for the first time to reveal the phenomenon of RTP in CDs, indicating that the hydrogen bonding of the PVA matrix and the C=O bonding on the surface of CDs can achieve cross-linking to form a stable rigid structure, which in turn facilitates the achievement of RTP. In 2014, Yan *et al.*<sup>86</sup> first observed the RTP of water-soluble CDs without a deoxidizer and other inducers in pure aqueous solution. They found that due to non-radiative electron transfer, phosphorescent emission can be quenched in the presence of iron ions ( $\text{Fe}^{3+}$ ), and then turned on by phosphate ions through strong interaction. In the presence of CD-based RTP, it is possible to easily avoid the interference of deoxidizers and other inducers necessary in conventional RTP detection, as well as self-fluorescence and composite matrix scattering light encountered in fluorescence spectrometry. In 2015, Gui *et al.*<sup>133</sup> for the first time reported RTP logic gates involving RTP emission based on carbon materials. They used capture ssDNA (cDNA) modified CDs and graphene oxide (GO). That is, firstly, the cDNA was combined with carboxyl group surface modified CDs ( $\text{HOOC-CDs}$ ) by carbodiimide chemistry, and then the cDNA-CD conjugates were adsorbed on the surface of GO through  $\pi$ - $\pi$  stacking interactions to form a cDNA-CD/GO complex. They verified the feasibility of the RTP logic gate based on the cDNA-CD/GO system. The logic gate is simple, easy to operate, and low-cost, does not require complex labeling and modification, and can be efficiently used in actual samples. In 2016, Jiang *et al.*<sup>111</sup> reported for the first time triple-mode emission (*i.e.*, photoluminescence (PL), up-conversion PL and RTP) on luminescent CDs prepared by compounding *m*-phenylenediamine and PVA. It is worth noting that this work is the first time to realize simultaneously triple-mode emission with a single material and put forward the advanced anti-counterfeiting of a triple authentication concept. And Li *et al.*<sup>47</sup> synthesized a highly efficient CD-based phosphorescent material by heating a mixture of urea and nitrogen doped CDs (NCDs) using one pot. It was found for the first time that new energy structures can be generated by C=N bonds on the NCD surface, and evidence that they are the origin of phosphorescence is proposed. Then, Tan *et al.*<sup>49</sup> prepared simple and large-scale nitrogen doped carbon quantum dots (N-CQDs) under microwave irradiation which was a new strategy to synthesize N-CQDs *via* using isophorone diisocyanate (IPDI) as a single carbon source. N-CQDs were dispersed in the polyurethane (PU) matrix, under the excitation of ultraviolet (UV) light, and they emitted not only FL, but also phosphorescence and DF at room temperature. In the following year, amphiphilic carbon quantum dots (ACDs) were also







Fig. 5 (A) Reprinted with permission from Long *et al.*<sup>91</sup> Copyright 2018, Wiley-VCH. (B) Reprinted with permission from Zheng *et al.*<sup>74</sup> Copyright 2022, Wiley-VCH. (C) Reprinted with permission from Li *et al.*<sup>77</sup> Copyright 2021, Royal Society of Chemistry. (D) Reprinted with permission from He *et al.*<sup>55</sup> Copyright 2020, Wiley-VCH. (E) Reprinted with permission from Liu *et al.*<sup>63</sup> Copyright 2017, Science. (F) Reprinted with permission from Shi *et al.*<sup>51</sup> Copyright 2018, Wiley-VCH. (G) Representative studies of CD-based RTP materials in each year.

successfully prepared by Tan *et al.* via treating oil-soluble N-doped carbon quantum dots by a one pot hydrothermal method.<sup>134</sup> The obtained ACDs may be homogeneously dispersed in PVA and the PU matrix. Furthermore, RTP can be recognized in these ACD based composites. This is the first time that ACDs realize phosphorescent emission in polymers, which

greatly broadens the research and application scope of CQDs. In 2017, Chen *et al.*<sup>87</sup> reported for the first time the aggregation-induced RTP of self-quenching-resistant nitrogen doped CD powder by structure design *via* using PVA-chains, and the potential application of the temperature sensor is preliminarily prospected. Jiang *et al.*<sup>53</sup> also reported a new method for

preparing room temperature long afterglow materials by covalently fixing CDs onto colloidal nanosilica ( $\text{nSiO}_2$ ). A CD-based long afterglow material (*i.e.*,  $\text{m-CDs@nSiO}_2$ ) is reported for the first time, and the material is suitable for room temperature, and can even be directly observed in an air-saturated aqueous medium. The results show that the long afterglow materials of  $\text{m-CDs@nSiO}_2$  have mainly delayed fluorescence properties and mixed partial phosphorescence. In addition, Joseph *et al.*<sup>62</sup> also showed the observation of RTP emitted by CDs embedded in a silica gel matrix at room temperature. CDs in silica gel showed a long phosphorescence lifetime of 1.8 s, which is the highest value of CDs in solid state matrices, and the phosphorescent emission is displayed in the white gamut region in the chromaticity diagram. As a type of inorganic porous material, zeolite has emerged as one of the most desirable materials for loading and encapsulating metal nanoparticles and luminescent quantum dots because of its three-dimensional ordered structure and strong thermal stability. In the same year, Liu *et al.*<sup>63</sup> embedded CDs in a family of zeolitic crystalline matrices *in situ* under solvothermal/hydrothermal conditions to prepare a novel category of CD-based TADF materials with ultra-long lifetimes and achieved high quantum yields (QYs) up to 52.14%. This work offers a new “dots-in-zeolites” scheme for the design and synthesis of innovative TADF materials, which may open the application of various delayed fluorescence in various fields. In 2018, He *et al.*<sup>43</sup> used electrospinning technology to incorporate CDs into PVA, and achieved the two goals of RTP and TADF. It was found for the first example of the CDs/polymer system that the ordered mesoporous structure of electrospun CDs/PVA nanofibers allows effective stabilization of the triplet state of CDs, thus realizing the RISC process of TADF. To date, this is the first time that TADF has been found in the CDs/polymer system. Jiang *et al.*<sup>131</sup> reported the first example of conversion of a fluorescence material to RTP with an external heat stimulus, that is using ethylenediamine and phosphoric acid as raw materials, fluorescent emissive polymer CDs were prepared by simple heat treatment and can produce unexpected ultra-long RTP. It was found that the doping of N and P elements may be critical to the RTP production of CDs. Similarly, Jiang *et al.*<sup>89</sup> again reported an ultra-long CD-based RTP material by microwave-assisted heating of an aqueous solution of ethanolamine and phosphoric acid which showed the longest RTP lifetime (1.46 s) for CD-based materials to date. Long *et al.*<sup>91</sup> reported for the first time fluorine–nitrogen co-doped CDs (FNCDs) possessing long-lived triple excited states which emit pH-stabilized blue fluorescence and pH-responsive green self-protected RTP. In 2019, Li *et al.*<sup>54</sup> proposed a reasonable strategy for a kind of silica-based composite using CDs ( $\text{CDs@SiO}_2$ ) in air saturated aqueous media for realizing ultra-long RTP. More importantly, they reported the first application in practical imaging of biological samples for CD-based RTP materials. Also, through one-step heat treatment of nitrogen doped CDs and boric acid (BA) ( $\text{N-CDs/BA}$ ), a universal method for activating RTP of both heteroatom-free and heteroatom-containing CDs was achieved.<sup>120</sup>  $\text{N-CDs/BA}$  exhibits the best phosphorescence lifetime of 2.26 s and a PQY of 17.5%,

representing the most advanced record for CD-based RTP materials to date. In addition, Su *et al.*<sup>92</sup> proposed a method of microwave synthesis of nitrogen and phosphorus co-doped CDs (P-CDs) *via* using triethanolamine as the carbon source and phosphoric acid as the dopant. The prepared P-CDs showed not only bright-blue fluorescence in aqueous solution, but also obvious green phosphorescence on filter paper. More importantly, this study successfully realized a dual-channel signal for the detection and analysis of the pH value by using P-CDs for the first time, and found that the RTP signal is more sensitive than the fluorescence signal, and thus may provide a wider linear range. In the same year, Yuan *et al.*<sup>135</sup> also demonstrated for the first time that the synthesized single-component white carbon nitride quantum dots (W-CNQDs) exhibit a double emission of blue-yellow fluorescence–phosphorescence. The W-CNQDs offered an overall photoluminescence quantum efficiency (PLQY) of 25%, which is the largest of any white light-emitting material reported so far. In 2020, using CD modified amorphous silica ( $\text{CDs-SiO}_2$ ) as the raw material, He *et al.*<sup>55</sup> realized RTP and TADF in the solid state and aqueous solution through a one-pot sol-gel methodology without the addition of any heavy atomic scramblers and the removal of dissolved oxygen. Importantly, the thermoluminescence spectra of the CD-based matrix were for the first time visualized and evaluated. Jiang *et al.*<sup>136</sup> reported for the first time a simple method to prepare CDs (*i.e.*, TA-CDs) with double emission, robustness and aggregation induced RTP properties. The study showed that the yellow RTP of TA-CD powder may be due to its aggregation. Liang *et al.*<sup>58</sup> used silica to confine water-soluble phosphorescent carbon nanodots (WSP-CNDs@silica) in their nanospace and realized the ultra-long and efficient phosphorescence of CNDs. The phosphorescence lifetime and quantum yield (QY) reached 1.86 s and 11.6%, respectively, which is the best value of water-soluble phosphorescence nanoparticles reported so far. It is shown that the silica shell outside of CDs restricts the rotation and vibration of the bonds in CDs, resulting in the long life and high efficiency phosphorescence of CDs. Park *et al.*<sup>76</sup> reported a new engineering approach to manage singlet-triplet energy splitting ( $\Delta E_{\text{ST}}$ ) in graphene quantum dots (GQDs)/graphene oxide quantum dots (GOQDs) through varying the ratio of oxygen-containing carbon to  $\text{sp}^2$  carbon ( $\gamma_{\text{OC}}$ ). This is the first time that GQDs are used as a long-life RTP and TADF material to demonstrate anti-counterfeiting and multi-level information security. Wang *et al.*<sup>94</sup> developed a one-step synthesis method with low cost, rapid processing and environmental protection for the fabrication of single-component white luminescence carbonated polymer dots (SW-CPDs) on a gram scale with high efficiency. The overall QY was as high as 41%, and that was the largest value ever recorded for solid-state fluorescent CDs. The results showed that the hybrid fluorescent/phosphorescent components promoted the emergence of white light emission. In addition, Zhang *et al.*<sup>66</sup> successfully achieved high-efficiency afterglow  $\text{CDs@zeolite}$  composite materials by simply grinding the solid raw material zeolite and precursor CDs at room temperature and then performing thermal crystallization of  $\text{CDs@zeolite}$  by a solvent-free thermal synthesis strategy. In this



method, CDs are embedded into the growing zeolite crystals with the maximum extent, and the non-radiative transition of CDs is surpassed by the strong host–guest interaction, and thus composite materials with ultra-long double emission of TADF and RTP are prepared, and have a lifetime of 1.7 s and 2.1 s, respectively, as well as a QY of 90.7% and a PQY of 24.4%, respectively. These values are at the top superiority level among CD-based PL materials, and thus, represent the majority of organic afterglow materials. What's more, in 2021, Li *et al.*<sup>79</sup> reported a method to prepare highly efficient RTP materials from crystalline heat-annealed CDs and BA composites which can induce amorphous to crystalline transition by grinding. This method can enable CDs to be uniformly embedded in BA crystals to the maximum extent, reduce the non-radiation attenuation of CDs, and promote the cross-connections between systems by suppressing the free vibration of CDs, thus generating strong RTP materials. The reported PQY is the highest (48%). It is well known that water-soluble red afterglow imaging agents have a great penetration depth and nondurable excitation characteristics which have potential application prospects in time-gated afterglow bioimaging. Thus, Liang *et al.*<sup>59</sup> reported a red afterglow imaging agent composed of Rhodamine B (RhB) and CNDs, which were confined in a hydrophilic silica shell to form CNDs-RhB@silica nanocomposites. CNDs-RhB@silica can achieve a luminescence lifetime and afterglow QY of 0.91 seconds and 3.56%, respectively, which is the best result for the red afterglow region. Liang *et al.*<sup>60</sup> also reported a time division duplex technology based on environmentally friendly CNDs with controllable luminescence lifetime. It was the first time they demonstrated that the time-division duplexing technique for CNDs and CNDs@silica is independent of the emission color and intensity depending on the phosphorescence lifetime under control. Water has been demonstrated to play an essential role in modulating the luminescence lifetime of CNDs by quenching triple excitons. In addition, Tan *et al.*<sup>104</sup> also reported a method to realize time-dependent phosphorescence colors in CDs, which were synthesized through a one pot hydrothermal method by using levofloxacin as the raw material. They realized a new type of time-dependent phosphorescence color that changed from orange to green in a very short time (1 s). In 2021, Zheng *et al.*<sup>137</sup> also reported a general approach in which effective radiative energy transfer can be applied to support the reabsorption of upconversion materials (UMs) into CD-based room temperature near-infrared excited multicolor afterglow materials (CDAMs). Please note that this is the first report on the multicolor afterglow of near-infrared excited in CDAMs. More importantly, this work provides a general route for constructing novel room-temperature afterglow materials with tunable excitation wavelengths. For the first time, Zhou *et al.*<sup>138</sup> proposed an approach for efficient energy transfer mediation to boost the RTP of CDs by incorporating pure phosphorescent CDs into the afterglow matrix. In this system of design, there is a significant increase in the emission intensity, RTP lifetime and emission time of CDs, and all CD-based materials emit visible phosphorescence for more than 20 seconds after UV excitation. In addition, Mo *et al.*<sup>139</sup> provided

the first example of visible light excited TADF in aqueous solution by confining the co-doping of CDs with fluorine and nitrogen in silica nanoparticles (F, NCDs@SiO<sub>2</sub>). Although there have been many reports on RTP materials, it is still a challenging task to realize ultra-long RTP in aqueous media, especially for CD-based materials. In 2022, Jiang *et al.*<sup>73</sup> developed a robust organic long persistent luminescence (OLPL) system with hour-level afterglow emissions through simple microwave-assisted heating of a mixture of m-CDs and urea. It is a very uncommon case of an OLPL system displaying hourly afterglow under ambient conditions, even for aqueous media. Further studies showed that the generation of covalent bonds between cyanuric acid and CDs played a key role in the afterglow presentation. Green preparation has always been the synthetic route pursued by everyone. At present, RTP materials are greatly developed. Nevertheless, it is a huge priority to achieve both multicolor and long wavelength RTP emission with favorable stability in CD-based RTP materials. Liang *et al.*<sup>140</sup> proposed a new and general “CDs-in-YOHF” scheme to yield multicolor and long wavelength RTP by confining different CDs to a Y(OH)<sub>x</sub>F<sub>3-x</sub>(YOHF) matrix. It should be noted that the RTP lifetime of the orange emissive CDs-o@YOHF is the longest in the reported single-CD-matrix composite materials with emission above 570 nm. Compared with the common representative matrices, the YOHF matrix is also proved to be more effective in protecting the long-wavelength triplet emission of CDs-o. Similarly, Mo *et al.*<sup>61</sup> reported a newly developed strategy to incorporate phosphorescent CD and fluorescent dyes into monodisperse silica nanoparticles below 20 nm to achieve multi-color long afterglow in aqueous solution. For the first time, CD-based multicolor long afterglow systems (green, yellow, orange and red) were fabricated in aqueous solution by cascaded Förster resonance energy transfer. Especially, under UV excitation, a prolonged red afterglow with a Stokes shift of 255 nm was developed. So far, there have been few studies on thermal stimulated response photoluminescence of CD-based materials. Xu *et al.*<sup>141</sup> reported for the first time a polymeric nanocomposite incorporating fluorinated CDs (FCDs) that can be efficiently synthesized in large quantities through the utilization of commercial water-soluble polymer sodium carboxymethylcellulose (CMCNa) as a stable matrix. The synthesized FCDs-CMCNa has bimodal emission, *i.e.*, both solid state fluorescence and in-room RTP. It is more interesting to note that FCDs-CMCNa exhibits special temperature-sensitive optical properties when the temperature is reduced from 300 K to 90 K. It exhibits an increase in fluorescence/phosphorescence intensity with decreasing temperature up to the switching point of 150 K, which then gradually decreases with decreasing temperature to 90 K. Later, Liu *et al.*<sup>142</sup> proposed a series of flexible dynamic ultra-long RTP polymer composites, which are illuminated by halogen doped CDs and have fully programmable emission. They had produced a transparent, flexible and fully programmable dynamic ultra-long RTP composite film with reliable gray-scale display ability from the synthesized RTP material for the first time. As can be seen, each year's contribution has grown year on year, indicating a steady stream of scholars working on CD-based





RTP materials with notable achievements. In each year of the prominent work represented, RTP of CDs was slowly developed in the initial stage, however, three years later, it was springing up. This indicates that as research progresses, a steady stream of findings is discovered that continue to advance the development of RTP for CDs.

To sum up, the outstanding work of CD-based RTP materials is growing every year. According to Fig. 2, we conducted statistical analysis on all the 166 retrieved papers and summarized the corresponding RTP emission wavelengths (it is worth noting that the number of wavelengths counted here is more than the number of papers published because some articles reported multicolor wavelengths), as shown in Fig. 4. According to the statistical results, the emission of CD-based RTP materials is mainly concentrated in the range of 500–550 nm (Fig. 6a), accounting for 40.68% of the total (Fig. 6b). In other words, the current CD-based RTP materials mainly emit green light. The second is blue to green emission with emission wavelengths concentrated between 450 and 500 nm, followed by yellow-orange emission with emission wavelengths concentrated between 550 and 600 nm. It can be seen that the achievable emission of CD-based RTP materials is mainly concentrated in the short wavelength (450–600 nm) region of visible light, while reports of long wavelength emission (>600 nm) are very rare. Certainly, the realization of long-wavelength emission from CD-based RTP materials, even extending into the near-infrared region, is the focus of current research and the key to enhancing and broadening their application areas. This is a challenging research problem which needs to be solved.

#### 4. Annual representative studies of phosphorescence lifetime in CD-based RTP materials

RTP materials have attracted much attention because of their great optical application potential. With the deepening of

research, researchers have made breakthroughs in CD-based RTP materials, such as multi-mode emission RTP materials,<sup>72,111</sup> multi-color RTP materials,<sup>48,75,120,140,143</sup> aqueous solution RTP materials,<sup>55,59,61,86</sup> multifunctional detection application RTP materials,<sup>43,92,134</sup> biocompatible RTP materials<sup>54</sup> and high PQY<sup>79,94,135</sup> and ultra-long phosphorescence life RTP materials.<sup>46,57,58,73,89,131</sup> However, it is still difficult to obtain RTP materials with simultaneous long-lifetime and high PQY. In addition, phosphorescence lifetime is one of the important parameters to measure CD-based RTP materials. Phosphorescence lifetime is a key feature of RTP materials, and ultra-long phosphorescence lifetime is central to the excellent performance of RTP materials. The key to achieving long phosphorescence lifetimes is the choice of the RTP material structure or the implementation of methods, such as the use of melt co-crystallisation<sup>125</sup> to immobilize CDs in the form of wrapping to achieve RTP (Fig. 7A), the utilization of rigid structural networks and the coexistence of covalent bonds<sup>57</sup> to immobilize CDs in a three-dimensional spatially confined way to achieve RTP (Fig. 7B), the adoption of porous space crystalline materials<sup>66</sup> to immobilize CDs by adsorption and intercalation to achieve RTP (Fig. 7C), the employment of polymers to covalently cross-link CDs<sup>45</sup> to achieve RTP (Fig. 7D), the employment of metal-organic frameworks with porous structures providing active sites<sup>80</sup> to immobilize CDs to achieve RTP (Fig. 7E), and the utilization of high strength rigid crystal structures<sup>72</sup> to immobilize CDs to achieve RTP (Fig. 7F). Each year's work has made corresponding outstanding contributions, from the initial millisecond level to the later second level, and then to the current hour level, which are major breakthroughs one after another. As shown in Fig. 7G, the best phosphorescent life of CD-based phosphorescent materials is shown in each year from the first discovery to the present. In 2013, Deng *et al.*<sup>42</sup> reported for the first time that the phosphorescence phenomenon of CDs in the PVA matrix was observed, and its average phosphorescence life was as high as ~380 ms. Then, in 2014, Yan *et al.*<sup>86</sup> reported for the first time



Fig. 6 (a) Distribution of phosphorescence emission of CD-based RTP. (b) The proportion of phosphorescence emission of CD-based RTP in the total number of reported articles.



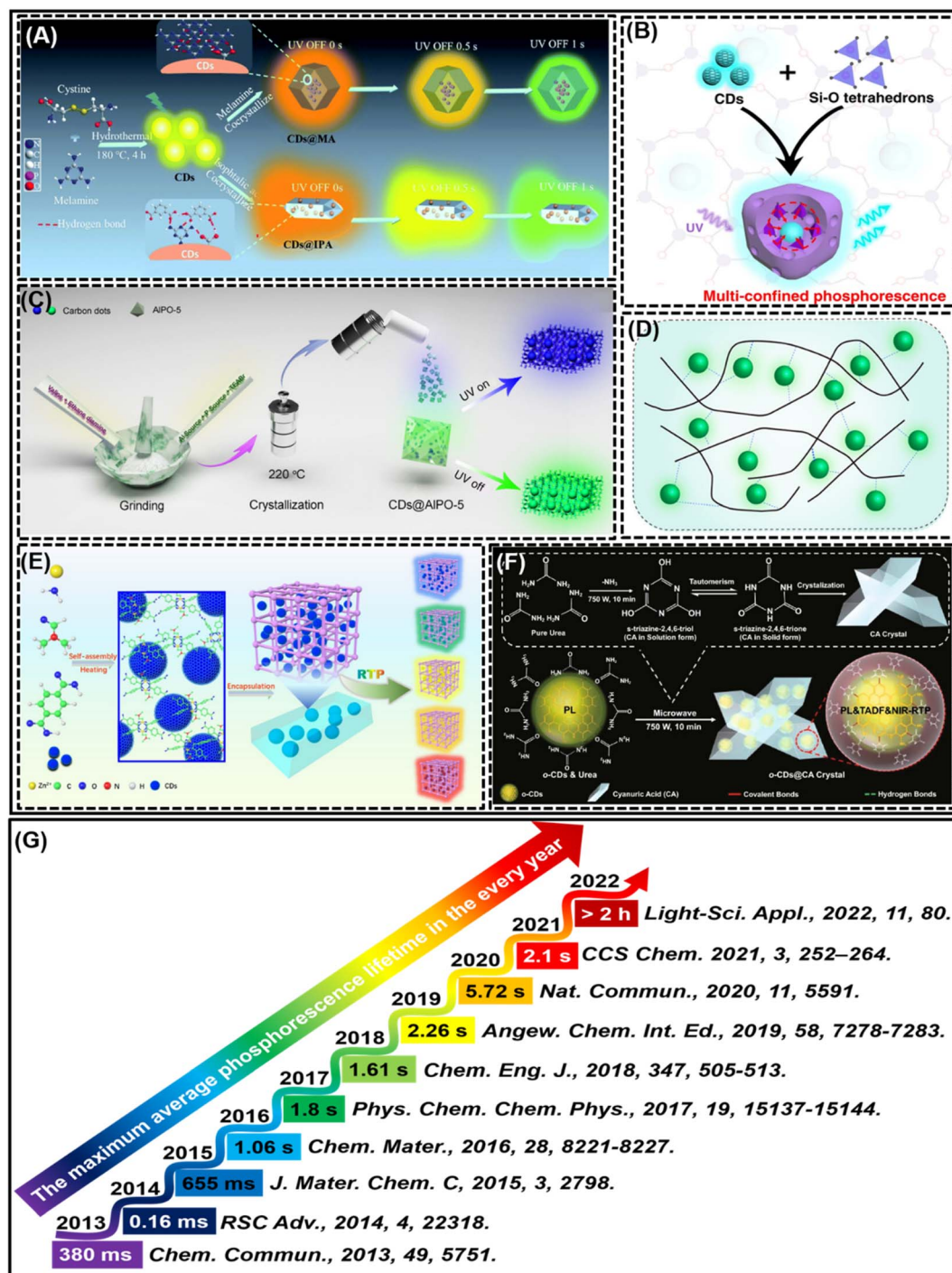


Fig. 7 (A) Reprinted with permission from Qu *et al.*<sup>125</sup> Copyright 2021, Royal Society of Chemistry. (B) Reprinted with permission from Sun *et al.*<sup>57</sup> Copyright 2019, Springer. (C) Reprinted with permission from Zhang *et al.*<sup>66</sup> Copyright 2020, Chinese Chemical Society. (D) Reprinted with permission from Cao *et al.*<sup>45</sup> Copyright 2022, American Chemical Society. (E) Reprinted with permission from Xu *et al.*<sup>80</sup> Copyright 2022, American Chemical Society. (F) Reprinted with permission from Wang *et al.*<sup>72</sup> Copyright 2021, Springer. (G) The longest phosphorescence lifetime of CD-based RTP materials in each year.

that the phosphorescence of CDs in pure aqueous solution was observed, but its average phosphorescence lifetime was only 0.16 ms. In 2015, Deng *et al.*<sup>46</sup> embedded CDs into a KAl(SO<sub>4</sub>)<sub>2</sub>·x(H<sub>2</sub>O) matrix to prepare composite powder of CDs, and presented long-lived RTP with an average phosphorescence life

of up to 655 ms. In 2016, Li *et al.*<sup>47</sup> prepared an efficient CD-based phosphorescent material, that is, NCDs were heated in one pot by treating a mixture of urea and NCDs, and then they were incorporated into the composite matrix. The resulting material had an ultra-long phosphorescent life of 1.06 s under

the excitation of 280 nm. In 2017, Joseph *et al.*<sup>62</sup> embedded CDs in a silica gel matrix to obtain an RTP material. The CDs showed strong blue fluorescence in aqueous dispersion and showed green afterglow when combined with silica gel. Under the excitation of 380 nm, the phosphorescent emission lifetime of the CDs is about 1.8 s, which is the highest value of CDs in a solid matrix. In 2018, He *et al.*<sup>43</sup> combined CDs with PVA *via* the help of electrospinning technology, and realized RTP and TADF at the same time. In addition, these nanofibers showed a longer average afterglow lifetime of 1.61 s and a visual recognition period of 9 s. In 2019, Li *et al.*<sup>43</sup> realized the preparation of RTP of CDs with or without heteroatom doping through a single-step thermal treatment of CDs and boric acid. This composite exhibits the highest phosphorescence lifetime of 2.26 s and a PQY of 17.5%, and this is the maximum record for CD-based RTP materials to date. In 2020, Sun *et al.*<sup>57</sup> obtained RTP materials with ultra-long life, high-level PQY and superior stability by rational design and fabrication of multi-constrained CDs. The designed multi-constrained CDs possess an ultra-long lifetime of 5.72 seconds, 26.36% PQY, and outstanding stability to strong oxidants, acids, bases, and polar solvents. In 2021, Yu *et al.*<sup>68</sup> systematically adapted the reaction parameters and host-guest interactions to achieve nine green RTP CDs-in-zeolite (CDs@zeolite) composites with engineering lifetimes ranging from 0.38 to 2.1 s under solvent-free conditions. In 2022, Jiang *et al.*<sup>73</sup> developed the first CD-based organic long persistent luminescence system with a duration of more than 1 h. A system based on CDs (named m-CDs@CA) is reported, which can be conveniently and efficiently fabricated through the utilization of a household microwave oven. What is even more impressive is that its long-term sustained luminescence may be noticed under ambient conditions, even in aqueous media. In summary, the extension of phosphorescence lifetimes has always been at the heart of scholars' pursuits, and shows that phosphorescence lifetimes occupy an irreplaceable and central position in the RTP of CDs, and are

a sign that CDs exhibit RTP properties. Progress in the field of research can be seen in the representative work each year, and in the advancement of scientific capabilities. Following on from the previous research, the phosphorescence lifetime of CD RTP has made a qualitative breakthrough, extending from the initial millisecond level to the hourly level, which provides favorable preconditions for the practical application of CDs RTP.

Phosphorescence lifetime is an important index to measure RTP materials, and the phosphorescence lifetime of CD-based RTP materials is also constantly developing. According to Fig. 2, the phosphorescence lifetime of the published CD-based RTP materials was statistically analyzed. As shown in Fig. 8a, CD-based RTP materials with different phosphorescence lifetimes have been reported one after another, but the main phosphorescence lifetimes are between 1 and 1000 ms. More obviously, the phosphorescence lifetime of most CD-based RTP materials is still at the millisecond level. Of course, there are also some outstanding performances, such as the existence of phosphorescence lifetime at the level of hours, but this is rare. According to the analysis of statistical data, the ratio of phosphorescence lifetime between 1 and 1000 ms accounts for 67.76%, which is a very high percentage, while the ratio between 1000 and 5000 ms reaches 25.66% (Fig. 8b). It can be seen that the preparation of CD-based phosphor materials with second phosphorescence lifetime is still in the stage of development. It is worth noting that CD-based RTP materials with all second phosphorescence lifetimes account for less than half of all reported CD-based RTP materials. This is a very terrible existence. Therefore, developing CD-based RTP materials with ultra-long phosphorescence lifetime is a hot spot and a difficult problem at present.

## 5. Applications

Realizing the final application is the value of a material. As new luminescent materials, CD-based RTP materials are no



Fig. 8 (a) Distribution of phosphorescence lifetime of CD-based RTP. (b) The proportion of phosphorescence lifetime of CD based-RTP in the total number of reported articles.

Table 3 Applications of CD-based RTP materials

| Application            |                         | Method  | Afterglow emission (nm) | Afterglow lifetime ( $\tau$ ) ms <sup>-1</sup> (298 K) | Remarks                  | Ref. |
|------------------------|-------------------------|---|-------------------------|--|--------------------------|------|
| Anti-counterfeiting    |                         | A composite film of m-CDs (CDs prepared from <i>m</i> -phenylenediamine) and polyvinyl alcohol (PVA)  | 500                     | 456  | CDs-PVA                  | 111  |
|                        |                         | Microwave-assisted heating of ethanolamine and phosphoric acid aqueous solution   | 535                     | 1460   | URTP CDs                 | 89   |
|                        |                         | <i>In situ</i> in the hydrothermal system by using an organic amine as the template and the precursor of the CDs and an inorganic crystalline framework as the matrix | 620                     | 10.94  | CDs@MnAPO-CJ50           | 81   |
|                        |                         | By one-step heat treatment of CDs and boric acid (BA)   | 490–570                 | 2260   | a-CDs/BA                 | 120  |
|                        |                         | One-step solvothermal treatment   | 455                     | 1210   | FNCDs                    | 91   |
|                        |                         | Hydrothermal treatment of trimellitic acid  | 560                     | 183.6  | TA-CDs                   | 136  |
|                        |                         | A hydrothermal reaction of succinic acid and diethylenetriamine   | 500–575                 | 880  | MP-CDs                   | 144  |
|                        |                         | Thermal-treated CDs into a PVA matrix   | 420–440                 | >100   | CD@PVA                   | 113  |
| Information encryption |                         | A hydrothermal treatment of nSiO <sub>2</sub> solution mixed with m-CD solution   | 470                     | 703  | m-CDs@nSiO <sub>2</sub>  | 53   |
|                        |                         | Using polyacid and diamine to synthesize PCDs through a one-step hydrothermal treatment   | 494                     | 658.11   | PCDs                     | 88   |
|                        |                         | A further heat treatment of the F-CD powder at a higher temperature   | 538                     | 1390   | F-CDs                    | 131  |
|                        |                         | By <i>in situ</i> embedding CDs within a series of zeolitic crystalline matrices under solvothermal/hydrothermal conditions   | 430                     | 350  | CDs@zeolite              | 63   |
|                        |                         | By utilizing CDs and melamine to construct hydrogen-bonded networks to form a polymer   | 529                     | 664  | M-CDs                    | 82   |
|                        |                         | By pyrolysis of citric acid and boric acid precursors   | 466–638                 | 113.9–581.76   | B-CD                     | 109  |
|                        |                         | One-pot hydrothermal treatment of levofloxacin  | 555/630                 | 354/237  | CD@paper                 | 104  |
|                        |                         | By confining CNDs in a silica encapsulation layer   | 520                     | 1860   | WSP-CNDs @ silica        | 58   |
| Biological imaging     |                         | Neutral red, KNO <sub>3</sub> , MgCl <sub>2</sub> and KH <sub>2</sub> PO <sub>4</sub> as precursors <i>via</i> the molten salt method                                 | 518/520                 | 546/616  | CD71                     | 180  |
|                        |                         | By confining the fluorine and nitrogen co-doped CDs in silica nanoparticles   | 500                     | 480  | F, NCDs@SiO <sub>2</sub> | 139  |
|                        |                         | One-step solvent-free catalytic assisted strategy   | 554                     | 243.2  | M-CDs                    | 108  |
|                        | WLED                    | A one-pot heat treatment of a mixture of urea and NCD   | 490                     | 1060   | HN powders               | 47   |
|                        | LEDs                    | CD-based composites were prepared by simply mixing CD solution and NaOH under constant stirring   | 480                     | 705  | CD/CA                    | 70   |
|                        | LEDs                    | <i>In situ</i> solvent-free thermal crystallization   | 530                     | 2100   | CDs@AlPO-5               | 66   |
|                        | WLED                    | One-step heat treatment of lycorine hydrochloride and boric acid  | 520                     | 1760   | CD@BA                    | 77   |
|                        | WLED                    | A one-step heat treatment process of urea and phosphoric acid aqueous solutions   | 495                     | 320  | SW-CPDs                  | 94   |
| Light-emitting diodes  | WLED                    | Encapsulating multicolor lignin-derived CDs and PVA into a delignified wood framework   | 505                     | 208.83   | LTW                      | 176  |
|                        | WLED                    | Through the solvothermal reaction of polyvinylpyrrolidone (PVP), urea, and seed CDs   | 501–596                 | 419  | CD powder                | 143  |
|                        | pH and Fe <sup>3+</sup> | One step hydrothermal   | 440                     | 0.16   | CD-based RTP             | 86   |



Table 3 (Contd.)

| Application         |                  | Method  | Afterglow emission (nm) | Afterglow lifetime ( $\tau$ ) ms <sup>-1</sup> (298 K) | Remarks       | Ref. |
|---------------------|------------------|---|-------------------------|--|---------------|------|
| Sensing detection   | pH               | Microwave strategy to synthesize P-CDs by using triethanolamine serving as the carbon source with phosphoric acid | 518                     | 820  | P-CDs         | 92   |
|                     | Fe <sup>3+</sup> | <i>In situ</i> green synthesis of CDs by using Schisandra chinensis polysaccharide as the only carbon source      | 510                     | 271.2  | CD/PVA        | 114  |
|                     | Humidity         | By combining chelate and hydrothermal methods   | 525                     | 1.34   | Eu-CDs/PV     | 186  |
|                     | Humidity         | By embedding biomass derived CDs into cellulose fibrils   | 560                     | 167.31   | CDs@Cellulose | 85   |
|                     | Fe <sup>3+</sup> | The CD solution mixed with CA under constant stirring   | 480                     | 687  | CD-CA         | 71   |
|                     | O <sub>2</sub>   | By intercalating the CD precursor (EDTA) into the LDH interlayer  | 525                     | 386.8  | CDs-LDHs      | 50   |
| Temperature sensing |                  | Hydrothermally synthesized using PVA and ethylene diamine   | 564                     | 13.4   | NCD           | 87   |
|                     |                  | By direct calcination of carbon sources (1,2,4-triaminobenzene) with inorganic salts                              | 506                     | 1280   | CDs@MP        | 124  |
|                     |                  | By incorporating CDs into poly(vinyl alcohol) (PVA) with the assistance of electrospinning technology             | 569                     | 1610   | CDs/PVA       | 43   |

exception. First of all, some CD-based materials have the characteristics of DF, which have the property of long life and can be used in the field of information security without prompt excitation. Secondly, some CD-based materials with DF characteristics have also been accompanied by RTP performances, and such multiple afterglow emission offers additional possibilities for information encryption and anti-counterfeiting applications. In addition, RTP materials based on CDs have strong sensitivity characteristics in some special detection, and are also used for response detection of ions, pH, temperature, time, fingerprint and so on. It is worth noting that CD-based RTP materials also have low toxicity and good biocompatibility, and also have great potential and development in the field of biological imaging. More importantly, CD-based RTP materials fully embody the characteristics of light-emitting materials, have good tunability, luminescence, stability and other optical properties, and have been greatly developed in the field of light-emitting diodes (LEDs). Table 3 summarizes some main applications of CD-based RTP materials. In addition, the special properties of CD based-RTP materials, such as excitation-related, temperature-related and afterglow color adjustable properties, enable them to build multi-level security defense in the field of information encryption and anti-counterfeiting. The long afterglow life of CD based-RTP provides new possibilities for easier identification of authenticity and information content. It allows significantly increased time to visualize cell states, enables speedy detection, and also facilitates bioimaging and detection. Generally speaking, the RTP material based on CDs possesses huge application prospects in the field of anti-counterfeiting,<sup>110,126,127,144–150</sup> information

encryption,<sup>113,115,118,119,121,123,128,151–160</sup> sensor detection,<sup>114,124,129,130,147,161–174</sup> LEDs,<sup>175–179</sup> biological imaging,<sup>134,180,181</sup> logic gates,<sup>133</sup> fluorescent ink<sup>112,182–184</sup> and other fields<sup>116,117,122,185–195</sup> with the properties of DF, TADF, long afterglow life and adjustable afterglow color.

However, the application of CD RTP is also limited by its own deficiencies. First, the clarity in the luminescence mechanism of CDs is lacking. Different types of CDs have been reported one after another since the development of CDs, but equally inconsistent types of luminescence mechanisms have emerged, which seriously affects the unified definition and future application of CDs and prevents a systematic unification. Secondly, the process for the preparation of RTPs for CDs is too harsh. The current implementation of RTP for CDs requires the assistance of a matrix, high temperature or multi-step synthesis, and the process requirements are too demanding and costly, limiting their preparation and application for large scale production. Then, the RTP emission wavelengths of CDs are too short-term. According to the reported articles, most of the RTP emission wavelengths of CDs are concentrated in the range of 480–550 nm, while there is relatively little RTP emission for long wavelengths (>550 nm), which severely limits the application of RTP characteristics of CDs for advanced information security and encryption. Finally, the PLQYs for CDs RTP are relatively low. There is an urgent need for green preparation of RTP CDs with high quality and high PLQY, especially with long wavelength emission. In the field of optoelectronic devices, especially for WLED applications, red emission is the key to achieving efficient WLEDs and strong luminescence is also the key factor to enhance device





performance, and the emission of current RTP CDs greatly hinders their application in optoelectronics. Thus, the current low PLQY and the emission of RTP CDs have greatly hindered their application in the field of optoelectronics.

## 6. Challenges and prospects

Although significant achievements in the synthesis and diversified application investigations of CD-based RTP composites have been made, there remain enormous challenges to face. The specific aspects are as follows:

First, since the discovery and development of CDs, the luminescence mechanism of CDs has always been questioned since it does not have a unified structure. At present, we can accept two main categories, namely, carbon core luminescence and surface state luminescence. Similarly, the luminescence of CD-based RTP materials, as a special property of CD luminescence, has not yet been clearly explained and defined. For the luminescence mechanism of CD-based RTP, there are different opinions, each with its own words. For example, it has been reported that CD-based RTP originates from C=N, C=O, C=F, hydrogen bonds, polymer matrices and so on. However, these remarks are all unilateral. Thus, it is essential to address systematically their mutual and distinctive features, as well as their structural evolution patterns during CD synthesis. At the same time, the formation process and luminescence mechanism of CD-based RTP are explored and summarized by combining some more advanced characterization technologies and theoretical calculations, so that future generations can better understand the luminescence mechanism of CD-based RTP materials.

Second, luminescence quantum efficiency is one of the important indicators to measure luminescent materials. As a new emerging carbon based fluorescent nanomaterial, the PLQY of CDs has always been a hot and difficult research topic, and improving the PLQYs of CDs has always been our goal. More importantly, the PQY of CD-based RTP materials is much lower than the PLQY of CD fluorescence, which makes improving the PQY of CD-based RTP materials an urgent need. In addition, compared with CD-based RTP materials, the DF characteristics of CDs require a smaller energy difference (between the excited singlet state and the excited triplet state), which will make the preparation of CD-based DF materials more difficult. Because this also requires that the spatial overlap between the HOMO and LOMO be very small, which in turn reduces the radiation transition rate and ultimately leads to a low PQY. However, reasonable structural design, purification and appropriate matrix selection are expected to solve the pressing problem of low PQY of CD-based RTP materials.

Third, the recognition ability of human eyes is limited. In the visible light region, the luminescence of CDs is mainly concentrated in the short wavelength region (<600 nm), and even the luminescence of CD-based RTP materials is mainly concentrated in the blue to green light range. These short wavelength lights are harmful to the human body. In addition, the luminescence of CD-based RTP materials is mainly concentrated in the solid state, and the luminescence in

solution is relatively less. These limitations have seriously hindered the application of CD-based RTP materials in multi-color displays and bio-imaging. Therefore, the development of CD-based RTP materials with a long wavelength and liquid phase luminescence has also become a hot spot and an unsolved problem in current research. But, it is expected to solve the problem of luminescence at long wavelengths and in the liquid phase by choosing suitable hydrophilic matrices and surface modification.

Fourth, the phosphorescence lifetime is also one of the important indicators to measure the performance of CD-based RTP materials. Currently, the phosphorescence lifetime of CD-based RTP materials is mainly concentrated at the second level, and it is only a few seconds to several tens of seconds. Regarding the long-lifetime research, there are still few reports on minute-level, and even hour-level phosphorescence lifetime researches. In addition, CD-based RTP materials with an ultra-long phosphorescence lifetime are expected to show application value in new fields, such as solar cells. In order to realize CD-based RTP materials with ultra-long phosphorescence lifetime, an important matrix selection is the key to solving the problem.

Finally, advanced synthesis methods are one of the key technologies for preparing high-quality CD-based RTP materials. At present, the synthesis route of CD-based RTP materials mainly relies on a two-step method, that is, a matrix-assisted synthesis route is adopted, CDs are synthesized first, and then encapsulated into a matrix to realize RTP. This synthesis method is complicated and inefficient. In addition, the stability of the synthesized CD-based RTP material is also not good. More importantly, in addition to cumbersome synthesis methods, complicated purification processes are also required in the process of realizing CD-based RTP, and the low repetition rate of these synthesis routes greatly limits its large-scale commercial application. Therefore, in order to solve a series of problems in the preparation process, one kind of excellent matrix with a simple and fast preparation method and high stability properties is the only choice.

In summary, CD-based RTP materials have many excellent properties such as low cost, low toxicity and tunable luminescence. It has some advantages unmatched by other RTP materials, and has become a rising star in the fields of anti-counterfeiting, information security, LEDs, sensor detection and so on. However, there are still some problems, such as unclear luminescence mechanism, low PQY, short luminescence wavelength, insufficient phosphorescence lifetime, and simple and convenient preparation methods. Therefore, as a new CD-based RTP material in the future, it will have advantages such as economy, liquid phase stability, long wavelength emission, multi-color emission, high PQY and environmental friendliness. At the same time, CD-based RTP materials can also be combined with other high-performance materials to obtain new composite materials and realize application value in new fields. It is hoped that through the continuous attempts and efforts of the broad masses of people, in modern society where opportunities and challenges coexist, CD-based RTP materials are expected to popularize people's



lives in the future and become the next generation of newly applied luminescent materials.

## Author contributions

All authors contributed to writing and revision of the manuscript.

## Conflicts of interest

The authors declare no competing interests.

## Acknowledgements

This work was supported by the National Natural Science Foundation of China (No. 21774098) and the 111 project (No. B18038).

## References

- X. Xu, R. Ray, Y. Gu, H. J. Ploehn, L. Gearheart, K. Raker and W. A. Scrivens, Electrophoretic analysis and purification of fluorescent single-walled carbon nanotube fragments, *J. Am. Chem. Soc.*, 2004, **126**(40), 12736–12737.
- Y. Han, X. Zhao, A. Vomiero, X. Gong and H. Zhao, Red and green-emitting biocompatible carbon quantum dots for efficient tandem luminescent solar concentrators, *J. Mater. Chem. C*, 2021, **9**(36), 12255–12262.
- M. Cao, X. Zhao and X. Gong, Ionic Liquid-Assisted Fast Synthesis of Carbon Dots with Strong Fluorescence and Their Tunable Multicolor Emission, *Small*, 2022, 2106683.
- H. Zhao, G. Liu, S. You, F. V. A. Camargo, M. Zavelani-Rossi, X. Wang, C. Sun, B. Liu, Y. Zhang, G. Han, A. Vomiero and X. Gong, Gram-scale synthesis of carbon quantum dots with a large Stokes shift for the fabrication of eco-friendly and high-efficiency luminescent solar concentrators, *Energy Environ. Sci.*, 2021, **14**(1), 396–406.
- J. Li and X. Gong, The Emerging Development of Multicolor Carbon Dots, *Small*, 2022, 2205099.
- B. Wang and S. Lu, The light of carbon dots: from mechanism to applications, *Matter*, 2022, **5**(1), 110–149.
- B. Wang, H. Song, X. Qu, J. Chang, B. Yang and S. Lu, Carbon dots as a new class of nanomedicines: opportunities and challenges, *Coord. Chem. Rev.*, 2021, **442**, 214010.
- S. Li, L. Li, H. Tu, H. Zhang, D. S. Silvester, C. E. Banks, G. Zou, H. Hou and X. Ji, The development of carbon dots: from the perspective of materials chemistry, *Mater. Today*, 2021, **51**, 188–207.
- C.-L. Shen, Q. Lou, K.-K. Liu, L. Dong and C.-X. Shan, Chemiluminescent carbon dots: synthesis, properties, and applications, *Nano Today*, 2020, **35**, 100954.
- J. Liu, R. Li and B. Yang, Carbon Dots: A New Type of Carbon-Based Nanomaterial with Wide Applications, *ACS Cent. Sci.*, 2020, **6**(12), 2179–2195.
- Z. Wei, W. Lu, X. Wang, J. Ni, U. H. Prova, C. Wang and G. Huang, Harnessing versatile dynamic carbon precursors for multi-color emissive carbon dots, *J. Mater. Chem. C*, 2022, **10**(6), 1932–1967.
- J. Chen, H. Zhao, Z. Li, X. Zhao and X. Gong, Highly efficient tandem luminescent solar concentrators based on eco-friendly copper iodide based hybrid nanoparticles and carbon dots, *Energy Environ. Sci.*, 2022, **15**(2), 799–805.
- X. Gong, S. Zheng, X. Zhao and A. Vomiero, Engineering high-emissive silicon-doped carbon nanodots towards efficient large-area luminescent solar concentrators, *Nano Energy*, 2022, **101**, 107617.
- J. Li, H. Zhao, X. Zhao and X. Gong, Red and yellow emissive carbon dots integrated tandem luminescent solar concentrators with significantly improved efficiency, *Nanoscale*, 2021, **13**(21), 9561–9569.
- J. Jia, W. Lu, Y. Gao, L. Li, C. Dong and S. Shuang, Recent advances in synthesis and applications of room temperature phosphorescence carbon dots, *Talanta*, 2021, **231**, 122350.
- J. Li, B. Wang, H. Zhang and J. Yu, Carbon Dots-in-Matrix Boosting Intriguing Luminescence Properties and Applications, *Small*, 2019, **15**(32), 1805504.
- K. Jiang, Y. Wang, Z. Li and H. Lin, Afterglow of carbon dots: mechanism, strategy and applications, *Mater. Chem. Front.*, 2020, **4**(2), 386–399.
- Y. Sun, X. Zhang, J. Zhuang, H. Zhang, C. Hu, M. Zheng, B. Lei and Y. Liu, The room temperature afterglow mechanism in carbon dots: current state and further guidance perspective, *Carbon*, 2020, **165**, 306–316.
- M. Lei, J. Zheng, Y. Yang, L. Yan, X. Liu and B. Xu, Carbon dots-based delayed fluorescent materials: mechanism, structural regulation and application, *iScience*, 2022, **25**(9), 104884.
- K. A. Fernando, S. Sahu, Y. Liu, W. K. Lewis, E. A. Gulians, A. Jafariyan, P. Wang, C. E. Bunker and Y. P. Sun, Carbon quantum dots and applications in photocatalytic energy conversion, *ACS Appl. Mater. Interfaces*, 2015, **7**(16), 8363–8376.
- X. T. Zheng, A. Ananthanarayanan, K. Q. Luo and P. Chen, Glowing graphene quantum dots and carbon dots: properties, syntheses, and biological applications, *Small*, 2015, **11**(14), 1620–1636.
- F. Yuan, S. Li, Z. Fan, X. Meng, L. Fan and S. Yang, Shining carbon dots: synthesis and biomedical and optoelectronic applications, *Nano Today*, 2016, **11**(5), 565–586.
- G. A. M. Hutton, B. C. M. Martindale and E. Reisner, Carbon dots as photosensitisers for solar-driven catalysis, *Chem. Soc. Rev.*, 2017, **46**(20), 6111–6123.
- Z. Peng, X. Han, S. Li, A. O. Al-Youbi, A. S. Bashammakh, M. S. El-Shahawi and R. M. Leblanc, Carbon dots: biomacromolecule interaction, bioimaging and nanomedicine, *Coord. Chem. Rev.*, 2017, **343**, 256–277.
- S. Zhu, Y. Song, J. Wang, H. Wan, Y. Zhang, Y. Ning and B. Yang, Photoluminescence mechanism in graphene quantum dots: Quantum confinement effect and surface/edge state, *Nano Today*, 2017, **13**, 10–14.
- C. Xia, S. Zhu, T. Feng, M. Yang and B. Yang, Evolution and Synthesis of Carbon Dots: From Carbon Dots to Carbonized Polymer Dots, *Adv. Sci.*, 2019, **6**(23), 1901316.



- 27 A. Xu, G. Wang, Y. Li, H. Dong, S. Yang, P. He and G. Ding, Carbon-Based Quantum Dots with Solid-State Photoluminescent: Mechanism, Implementation, and Application, *Small*, 2020, **16**(48), 2004621.
- 28 L. Ai, Y. Yang, B. Wang, J. Chang, Z. Tang, B. Yang and S. Lu, Insights into photoluminescence mechanisms of carbon dots: advances and perspectives, *Sci. Bull.*, 2021, **66**(8), 839–856.
- 29 C. He, P. Xu, X. Zhang and W. Long, The synthetic strategies, photoluminescence mechanisms and promising applications of carbon dots: current state and future perspective, *Carbon*, 2022, **186**, 91–127.
- 30 J. Li, H. Zhao, X. Zhao and X. Gong, Boosting efficiency of luminescent solar concentrators using ultra-bright carbon dots with large Stokes shift, *Nanoscale Horiz.*, 2022, **8**(1), 83–94.
- 31 M. Cao, X. Zhao and X. Gong, Achieving High-Efficiency Large-Area Luminescent Solar Concentrators, *JACS Au*, 2023, **3**(1), 25–35.
- 32 J. Li and X. Gong, One-step large-scale fabricating aggregation-induced emission carbon dots with strong solid-state fluorescence emission, *Mater. Today Chem.*, 2022, **26**, 101255.
- 33 Y. Wu, J. Li, X. Zhao and X. Gong, Nickel-doped carbon dots with enhanced and tunable multicolor fluorescence emission for multicolor light-emitting diodes, *Carbon*, 2023, **201**, 796–804.
- 34 W. Li, M. Wu, H. Jiang, L. Yang, C. Liu and X. Gong, Carbon dots/ZnO quantum dots composite-based white phosphors for white light-emitting diodes, *Chem. Commun.*, 2022, **58**(12), 1910–1913.
- 35 H.-x. Kang, J.-x. Zheng, X.-g. Liu and Y.-z. Yang, Phosphorescent carbon dots: microstructure design, synthesis and applications, *New Carbon Mater.*, 2021, **36**(4), 649–664.
- 36 X. Wei, J. Yang, L. Hu, Y. Cao, J. Lai, F. Cao, J. Gu and X. Cao, Recent advances in room temperature phosphorescent carbon dots: preparation, mechanism, and applications, *J. Mater. Chem. C*, 2021, **9**(13), 4425–4443.
- 37 T. Yuan, T. Meng, Y. Shi, X. Song, W. Xie, Y. Li, X. Li, Y. Zhang and L. Fan, Toward phosphorescent and delayed fluorescent carbon quantum dots for next-generation electroluminescent displays, *J. Mater. Chem. C*, 2022, **10**(7), 2333–2348.
- 38 C. Zheng, S. Tao and B. Yang, Polymer-Structure-Induced Room-Temperature Phosphorescence of Carbon Dot Materials, *Small Struct.*, 2023, 2200327.
- 39 D. Wang, Z. Lu, X. Qin, Z. Zhang, Y. e. Shi, J. W. Y. Lam, Z. Wang and B. Z. Tang, Boric Acid-Activated Room-Temperature Phosphorescence and Thermally Activated Delayed Fluorescence for Efficient Solid-State Photoluminescence Materials, *Adv. Opt. Mater.*, 2022, **10**(18), 2200629.
- 40 C. Zhang, H. Wang, X. Lan, Y. E. Shi and Z. Wang, Modulating Emission of Nonconventional Luminophores from Nonemissive to Fluorescence and Room-Temperature Phosphorescence via Dehydration-Induced Through-Space Conjugation, *J. Phys. Chem. Lett.*, 2021, **12**(5), 1413–1420.
- 41 S. J. Zhu, Y. B. Song, X. H. Zhao, J. R. Shao, J. H. Zhang and B. Yang, The photoluminescence mechanism in carbon dots (graphene quantum dots, carbon nanodots, and polymer dots): current state and future perspective, *Nano Res.*, 2015, **8**(2), 355–381.
- 42 Y. Deng, D. Zhao, X. Chen, F. Wang, H. Song and D. Shen, Long lifetime pure organic phosphorescence based on water soluble carbon dots, *Chem. Commun.*, 2013, **49**(51), 5751–5753.
- 43 J. He, Y. He, Y. Chen, X. Zhang, C. Hu, J. Zhuang, B. Lei and Y. Liu, Construction and multifunctional applications of carbon dots/PVA nanofibers with phosphorescence and thermally activated delayed fluorescence, *Chem. Eng. J.*, 2018, **347**, 505–513.
- 44 L. Zhai, X.-M. Ren and Q. Xu, Carbogenic  $\pi$ -conjugated domains as the origin of afterglow emissions in carbon dot-based organic composite films, *Mater. Chem. Front.*, 2021, **5**(11), 4272–4279.
- 45 Q. Cao, K. K. Liu, Y. C. Liang, S. Y. Song, Y. Deng, X. Mao, Y. Wang, W. B. Zhao, Q. Lou and C. X. Shan, Brighten Triplet Excitons of Carbon Nanodots for Multicolor Phosphorescence Films, *Nano Lett.*, 2022, **22**(10), 4097–4105.
- 46 X. Dong, L. Wei, Y. Su, Z. Li, H. Geng, C. Yang and Y. Zhang, Efficient long lifetime room temperature phosphorescence of carbon dots in a potash alum matrix, *J. Mater. Chem. C*, 2015, **3**(12), 2798–2801.
- 47 Q. Li, M. Zhou, Q. Yang, Q. Wu, J. Shi, A. Gong and M. Yang, Efficient Room-Temperature Phosphorescence from Nitrogen-Doped Carbon Dots in Composite Matrices, *Chem. Mater.*, 2016, **28**(22), 8221–8227.
- 48 C. Lin, Y. Zhuang, W. Li, T. L. Zhou and R. J. Xie, Blue, green, and red full-color ultralong afterglow in nitrogen-doped carbon dots, *Nanoscale*, 2019, **11**(14), 6584–6590.
- 49 J. Tan, R. Zou, J. Zhang, W. Li, L. Zhang and D. Yue, Large-scale synthesis of N-doped carbon quantum dots and their phosphorescence properties in a polyurethane matrix, *Nanoscale*, 2016, **8**(8), 4742–4747.
- 50 L. Q. Bai, N. Xue, X. R. Wang, W. Y. Shi and C. Lu, Activating efficient room temperature phosphorescence of carbon dots by synergism of orderly non-noble metals and dual structural confinements, *Nanoscale*, 2017, **9**(20), 6658–6664.
- 51 W. Shi, J. Yao, L. Bai and C. Lu, Defect-Stabilized Triplet State Excitons: Toward Ultralong Organic Room-Temperature Phosphorescence, *Adv. Funct. Mater.*, 2018, **28**(52), 1804961.
- 52 X. Kong, X. Wang, H. Cheng, Y. Zhao and W. Shi, Activating room temperature phosphorescence by organic materials using synergistic effects, *J. Mater. Chem. C*, 2019, **7**(2), 230–236.
- 53 K. Jiang, Y. Wang, C. Cai and H. Lin, Activating Room Temperature Long Afterglow of Carbon Dots via Covalent Fixation, *Chem. Mater.*, 2017, **29**(11), 4866–4873.
- 54 W. Li, S. Wu, X. Xu, J. Zhuang, H. Zhang, X. Zhang, C. Hu, B. Lei, C. F. Kaminski and Y. Liu, Carbon Dot-Silica



- Nanoparticle Composites for Ultralong Lifetime Phosphorescence Imaging in Tissue and Cells at Room Temperature, *Chem. Mater.*, 2019, **31**(23), 9887–9894.
- 55 J. He, Y. Chen, Y. He, X. Xu, B. Lei, H. Zhang, J. Zhuang, C. Hu and Y. Liu, Anchoring Carbon Nanodots onto Nanosilica for Phosphorescence Enhancement and Delayed Fluorescence Nascence in Solid and Liquid States, *Small*, 2020, **16**(49), 2005228.
  - 56 Y. Sun, J. Liu, X. Pang, X. Zhang, J. Zhuang, H. Zhang, C. Hu, M. Zheng, B. Lei and Y. Liu, Temperature-responsive conversion of thermally activated delayed fluorescence and room-temperature phosphorescence of carbon dots in silica, *J. Mater. Chem. C*, 2020, **8**(17), 5744–5751.
  - 57 Y. Sun, S. Liu, L. Sun, S. Wu, G. Hu, X. Pang, A. T. Smith, C. Hu, S. Zeng, W. Wang, Y. Liu and M. Zheng, Ultralong lifetime and efficient room temperature phosphorescent carbon dots through multi-confinement structure design, *Nat. Commun.*, 2020, **11**(1), 5591.
  - 58 Y.-C. Liang, S.-S. Gou, K.-K. Liu, W.-J. Wu, C.-Z. Guo, S.-Y. Lu, J.-H. Zang, X.-Y. Wu, Q. Lou, L. Dong, Y.-F. Gao and C.-X. Shan, Ultralong and efficient phosphorescence from silica confined carbon nanodots in aqueous solution, *Nano Today*, 2020, **34**, 100900.
  - 59 Y. C. Liang, Q. Cao, K. K. Liu, X. Y. Peng, L. Z. Sui, S. P. Wang, S. Y. Song, X. Y. Wu, W. B. Zhao, Y. Deng, Q. Lou, L. Dong and C. X. Shan, Phosphorescent Carbon-Nanodots-Assisted Forster Resonant Energy Transfer for Achieving Red Afterglow in an Aqueous Solution, *ACS Nano*, 2021, **15**(10), 16242–16254.
  - 60 Y. C. Liang, K. K. Liu, X. Y. Wu, Q. Lou, L. Z. Sui, L. Dong, K. J. Yuan and C. X. Shan, Lifetime-Engineered Carbon Nanodots for Time Division Duplexing, *Adv. Sci.*, 2021, **8**(6), 2003433.
  - 61 L. Q. Mo, H. Liu, Z. M. Liu, X. K. Xu, B. F. Lei, J. L. Zhuang, Y. L. Liu and C. F. Hu, Cascade Resonance Energy Transfer for the Construction of Nanoparticles with Multicolor Long Afterglow in Aqueous Solutions for Information Encryption and Bioimaging, *Adv. Opt. Mater.*, 2022, **10**(10), 2102666.
  - 62 J. Joseph and A. A. Anappara, Cool white, persistent room-temperature phosphorescence in carbon dots embedded in a silica gel matrix, *Phys. Chem. Chem. Phys.*, 2017, **19**(23), 15137–15144.
  - 63 J. Liu, N. Wang, Y. Yu, Y. Yan, H. Zhang, J. Li and J. Yu, Carbon dots in zeolites: A new class of thermally activated delayed fluorescence materials with ultralong lifetimes, *Sci. Adv.*, 2017, **3**(5), 1603171.
  - 64 B. Wang, Y. Mu, H. Zhang, H. Shi, G. Chen, Y. Yu, Z. Yang, J. Li and J. Yu, Red Room-Temperature Phosphorescence of CDs@Zeolite Composites Triggered by Heteroatoms in Zeolite Frameworks, *ACS Cent. Sci.*, 2019, **5**(2), 349–356.
  - 65 J. Liu, H. Zhang, N. Wang, Y. Yu, Y. Cui, J. Li and J. Yu, Template-Modulated Afterglow of Carbon Dots in Zeolites: Room-Temperature Phosphorescence and Thermally Activated Delayed Fluorescence, *ACS Mater. Lett.*, 2019, **1**(1), 58–63.
  - 66 H. Zhang, K. Liu, J. Liu, B. Wang, C. Li, W. Song, J. Li, L. Huang and J. Yu, Carbon Dots-in-Zeolite via In-Situ Solvent-Free Thermal Crystallization: Achieving High-Efficiency and Ultralong Afterglow Dual Emission, *CCS Chem.*, 2020, **2**(3), 118–127.
  - 67 X. Yu, K. Liu, H. Zhang, B. Wang, W. Ma, J. Li and J. Yu, Carbon Dots-in-EuAPO-5 Zeolite: Triple-Emission for Multilevel Luminescence Anti-Counterfeiting, *Small*, 2021, **17**(46), 2103374.
  - 68 X. Yu, K. Liu, H. Zhang, B. Wang, G. Yang, J. Li and J. Yu, Lifetime-Engineered Phosphorescent Carbon Dots-in-Zeolite Composites for Naked-Eye Visible Multiplexing, *CCS Chem.*, 2021, **3**(12), 252–264.
  - 69 H. Liu, F. Wang, Y. Wang, J. Mei and D. Zhao, Whispering Gallery Mode Laser from Carbon Dot-NaCl Hybrid Crystals, *ACS Appl. Mater. Interfaces*, 2017, **9**(21), 18248–18253.
  - 70 J. Tan, Y. Ye, X. Ren, W. Zhao and D. Yue, High pH-induced efficient room-temperature phosphorescence from carbon dots in hydrogen-bonded matrices, *J. Mater. Chem. C*, 2018, **6**(29), 7890–7895.
  - 71 Q. Li, M. Zhou, M. Yang, Q. Yang, Z. Zhang and J. Shi, Induction of long-lived room temperature phosphorescence of carbon dots by water in hydrogen-bonded matrices, *Nat. Commun.*, 2018, **9**(1), 734.
  - 72 Y. Wang, K. Jiang, J. Du, L. Zheng, Y. Li, Z. Li and H. Lin, Green and Near-Infrared Dual-Mode Afterglow of Carbon Dots and Their Applications for Confidential Information Readout, *Nano Micro Lett.*, 2021, **13**(1), 198.
  - 73 K. Jiang, Y. Wang, C. Lin, L. Zheng, J. Du, Y. Zhuang, R. Xie, Z. Li and H. Lin, Enabling robust and hour-level organic long persistent luminescence from carbon dots by covalent fixation, *Light: Sci. Appl.*, 2022, **11**(1), 80.
  - 74 Y. Zheng, Q. Zhou, Y. Yang, X. Chen, C. Wang, X. Zheng, L. Gao and C. Yang, Full-Color Long-Lived Room Temperature Phosphorescence in Aqueous Environment, *Small*, 2022, **18**(19), 2201223.
  - 75 L. A. Diaz-Torres, C. Gomez-Solis, J. Oliva, C. R. García, A. I. Oliva, C. Angeles-Chavez and G. A. Hirata, Long-lasting green, yellow, and red phosphorescence of carbon dots embedded on ZnAl<sub>2</sub>O<sub>4</sub> nanoparticles synthesized by a combustion method, *J. Phys. D: Appl. Phys.*, 2018, **51**(41), 415104.
  - 76 M. Park, H. S. Kim, H. Yoon, J. Kim, S. Lee, S. Yoo and S. Jeon, Controllable Singlet-Triplet Energy Splitting of Graphene Quantum Dots through Oxidation: From Phosphorescence to TADF, *Adv. Mater.*, 2020, **32**(31), 2000936.
  - 77 Q. Li, Y. Li, S. Meng, J. Yang, Y. Qin, J. Tan and S. Qu, Achieving 46% efficient white-light emissive carbon dot-based materials by enhancing phosphorescence for single-component white-light-emitting diodes, *J. Mater. Chem. C*, 2021, **9**(21), 6796–6801.
  - 78 W. He, X. Sun and X. Cao, Construction and Multifunctional Applications of Visible-Light-Excited Multicolor Long Afterglow Carbon Dots/Boron Oxide Composites, *ACS Sustainable Chem. Eng.*, 2021, **9**(12), 4477–4486.





- 79 Q. Li, Z. Zhao, S. Meng, Y. Li, Y. Zhao, B. Zhang, Z. Tang, J. Tan and S. Qu, Ultra-strong phosphorescence with 48% quantum yield from grinding treated thermal annealed carbon dots and boric acid composite, *SmartMat*, 2021, 3(2), 260–268.
- 80 B. Xu, Z. Wang, J. Shen, J. Li, Y. Jia, T. Jiang, Z. Gao, X. Wang and X. Meng, Metal–Organic Framework-Activated Full-Color Room-Temperature Phosphorescent Carbon Dots with a Wide Range of Tunable Lifetimes for 4D Coding Applications, *J. Phys. Chem. C*, 2022, 126(28), 11701–11708.
- 81 B. Wang, Y. Yu, H. Zhang, Y. Xuan, G. Chen, W. Ma, J. Li and J. Yu, Carbon Dots in a Matrix: Energy-Transfer-Enhanced Room-Temperature Red Phosphorescence, *Angew. Chem., Int. Ed. Engl.*, 2019, 58(51), 18443–18448.
- 82 Y. Gao, H. Zhang, Y. Jiao, W. Lu, Y. Liu, H. Han, X. Gong, S. Shuang and C. Dong, Strategy for Activating Room-Temperature Phosphorescence of Carbon Dots in Aqueous Environments, *Chem. Mater.*, 2019, 31(19), 7979–7986.
- 83 Y. Deng, P. Li, H. Jiang, X. Ji and H. Li, Tunable afterglow luminescence and triple-mode emissions of thermally activated carbon dots confined within nanoclays, *J. Mater. Chem. C*, 2019, 7(43), 13640–13646.
- 84 Y. Liu, X. Huang, Z. Niu, D. Wang, H. Gou, Q. Liao, K. Xi, Z. An and X. Jia, Photo-induced ultralong phosphorescence of carbon dots for thermally sensitive dynamic patterning, *Chem. Sci.*, 2021, 12(23), 8199–8206.
- 85 P. Wang, D. Zheng, S. Liu, M. Luo, J. Li, S. Shen, S. Li, L. Zhu and Z. Chen, Producing long afterglow by cellulose confinement effect: a wood-inspired design for sustainable phosphorescent materials, *Carbon*, 2021, 171, 946–952.
- 86 X. Yan, J.-L. Chen, M.-X. Su, F. Yan, B. Li and B. Di, Phosphate-containing metabolites switch on phosphorescence of ferric ion engineered carbon dots in aqueous solution, *RSC Adv.*, 2014, 4(43), 22318–22323.
- 87 Y. Chen, J. He, C. Hu, H. Zhang, B. Lei and Y. Liu, Room temperature phosphorescence from moisture-resistant and oxygen-barred carbon dot aggregates, *J. Mater. Chem. C*, 2017, 5(25), 6243–6250.
- 88 S. Tao, S. Lu, Y. Geng, S. Zhu, S. A. T. Redfern, Y. Song, T. Feng, W. Xu and B. Yang, Design of Metal-Free Polymer Carbon Dots: A New Class of Room-Temperature Phosphorescent Materials, *Angew. Chem., Int. Ed. Engl.*, 2018, 57(9), 2393–2398.
- 89 K. Jiang, Y. Wang, X. Gao, C. Cai and H. Lin, Facile, Quick, and Gram-Scale Synthesis of Ultralong-Lifetime Room-Temperature-Phosphorescent Carbon Dots by Microwave Irradiation, *Angew. Chem., Int. Ed. Engl.*, 2018, 57(21), 6216–6220.
- 90 Y. Gao, H. Han, W. Lu, Y. Jiao, Y. Liu, X. Gong, M. Xian, S. Shuang and C. Dong, Matrix-Free and Highly Efficient Room-Temperature Phosphorescence of Nitrogen-Doped Carbon Dots, *Langmuir*, 2018, 34(43), 12845–12852.
- 91 P. Long, Y. Feng, C. Cao, Y. Li, J. Han, S. Li, C. Peng, Z. Li and W. Feng, Self-Protective Room-Temperature Phosphorescence of Fluorine and Nitrogen Codoped Carbon Dots, *Adv. Funct. Mater.*, 2018, 28(37), 1800791.
- 92 Q. Su, C. Lu and X. Yang, Efficient room temperature phosphorescence carbon dots: Information encryption and dual-channel pH sensing, *Carbon*, 2019, 152, 609–615.
- 93 H. Li, S. Ye, J. Guo, J. Kong, J. Song, Z. Kang and J. Qu, The design of room-temperature-phosphorescent carbon dots and their application as a security ink, *J. Mater. Chem. C*, 2019, 7(34), 10605–10612.
- 94 Z. Wang, Y. Liu, S. Zhen, X. Li, W. Zhang, X. Sun, B. Xu, X. Wang, Z. Gao and X. Meng, Gram-Scale Synthesis of 41% Efficient Single-Component White-Light-Emissive Carbonized Polymer Dots with Hybrid Fluorescence/Phosphorescence for White Light-Emitting Diodes, *Adv. Sci.*, 2020, 7(4), 1902688.
- 95 B. Wang, X. Yuan, X. Lv, Y. Mei, H. Peng, L. Li, Y. Guo, J. Du, B. Zheng and D. Xiao, Carbon dots-based room-temperature phosphorescent test strip: visual and convenient water detection in organic solvents, *Dyes Pigm.*, 2021, 189, 109226.
- 96 W.-S. Zou, T. Chen, D. Lin, W.-I. Kong, W. Li, F. Xie, Q. Qu, Y. Wang and C. Jiang, Amorphization of Purely Organic Phosphors into Carbon Dots to Activate Matrix-Free Room-Temperature Phosphorescence for Multiple Applications, *ACS Appl. Electron. Mater.*, 2021, 3(6), 2661–2670.
- 97 P. Liu, C. Liu, J. Chen and B. Wang, Facile Synthesis of Matrix-Free Room-Temperature Phosphorescent Nitrogen-Doped Carbon Dots and Their Application as Security Inks, *Macromol. Mater. Eng.*, 2021, 306(10), 2100339.
- 98 B. Zhao, R. Yu, K. Xu, C. Zou, H. Ma, S. Qu and Z. a. Tan, Highly efficient carbon dot-based room-temperature fluorescence–phosphorescence dual emitter, *J. Mater. Chem. C*, 2021, 9(43), 15577–15582.
- 99 S. Pagidi, H. K. Sadhanala, K. Sharma and A. Gedanken, One-Pot Synthesis of Deep Blue Hydrophobic Carbon Dots with Room Temperature Phosphorescence, White Light Emission, and Explosive Sensor, *Adv. Electron. Mater.*, 2021, 8(4), 2100969.
- 100 L. Zhang, M. Wu, Z. Wang, H. Guo, L. Wang and M. Wu, Phosphorescence Tuning of Fluorine, Oxygen-Codoped Carbon Dots by Substrate Engineering, *ACS Sustainable Chem. Eng.*, 2021, 9(48), 16262–16269.
- 101 Q. Su and X. Yang, Promoting Room Temperature Phosphorescence through Electron Transfer from Carbon Dots to Promethazine, *ACS Appl. Mater. Interfaces*, 2021, 13(34), 41238–41248.
- 102 F. Liu, Z. Li, Y. Li, Y. Feng and W. Feng, Room-temperature phosphorescent fluorine-nitrogen co-doped carbon dots: information encryption and anti-counterfeiting, *Carbon*, 2021, 181, 9–15.
- 103 Z. Wang, J. Shen, B. Xu, Q. Jiang, S. Ming, L. Yan, Z. Gao, X. Wang, C. Zhu and X. Meng, Thermally Driven Amorphous-Crystalline Phase Transition of Carbonized Polymer Dots for Multicolor Room-Temperature Phosphorescence, *Adv. Opt. Mater.*, 2021, 9(16), 2100421.



- 104 J. Tan, Q. Li, S. Meng, Y. Li, J. Yang, Y. Ye, Z. Tang, S. Qu and X. Ren, Time-Dependent Phosphorescence Colors from Carbon Dots for Advanced Dynamic Information Encryption, *Adv. Mater.*, 2021, **33**(16), 2006781.
- 105 J. Zhu, J. Hu, Q. Hu, X. Zhang, E. V. Ushakova, K. Liu, S. Wang, X. Chen, C. Shan, A. L. Rogach and X. Bai, White Light Afterglow in Carbon Dots Achieved via Synergy between the Room-Temperature Phosphorescence and the Delayed Fluorescence, *Small*, 2022, **18**(1), 2105415.
- 106 S. Cui, B. Wang, Y. Zan, Z. Shen, S. Liu, W. Fang, X. Yan, Y. Li and L. Chen, Colorful, time-dependent carbon dot-based afterglow with ultralong lifetime, *Chem. Eng. J.*, 2022, **431**, 133373.
- 107 Y. Liu, X. Kang, Y. Xu, Y. Li, S. Wang, C. Wang, W. Hu, R. Wang and J. Liu, Modulating the Carbonization Degree of Carbon Dots for Multicolor Afterglow Emission, *ACS Appl. Mater. Interfaces*, 2022, **14**(19), 22363–22371.
- 108 J. Bai, G. Yuan, X. Chen, L. Zhang, Y. Zhu, X. Wang and L. Ren, Simple Strategy for Scalable Preparation Carbon Dots: RTP, Time-Dependent Fluorescence, and NIR Behaviors, *Adv. Sci.*, 2022, **9**(5), 2104278.
- 109 Y. Ding, X. Wang, M. Tang and H. Qiu, Tailored Fabrication of Carbon Dot Composites with Full-Color Ultralong Room-Temperature Phosphorescence for Multidimensional Encryption, *Adv. Sci.*, 2022, **9**(3), 2103833.
- 110 Y. Liu, C. Zheng and B. Yang, Phosphorus and Nitrogen Codoped Carbonized Polymer Dots with Multicolor Room Temperature Phosphorescence for Anticounterfeiting Painting, *Langmuir*, 2022, **38**(27), 8304–8311.
- 111 K. Jiang, L. Zhang, J. Lu, C. Xu, C. Cai and H. Lin, Triple-Mode Emission of Carbon Dots: Applications for Advanced Anti-Counterfeiting, *Angew. Chem., Int. Ed. Engl.*, 2016, **55**(25), 7231–7235.
- 112 X. Wu, W. Li, P. Wu, C. Ma, Y. Liu, M. Xu and S. Liu, Long-Lived Room-Temperature Phosphorescent Nitrogen-Doped CQDs/PVA Composites: Fabrication, Characterization and Application, *Eng. Sci.*, 2018, **4**, 111–118.
- 113 Z. Tian, D. Li, E. V. Ushakova, V. G. Maslov, D. Zhou, P. Jing, D. Shen, S. Qu and A. L. Rogach, Multilevel Data Encryption Using Thermal-Treatment Controlled Room Temperature Phosphorescence of Carbon Dot/Polyvinylalcohol Composites, *Adv. Sci.*, 2018, **5**(9), 1800795.
- 114 X. Wu, C. Ma, J. Liu, Y. Liu, S. Luo, M. Xu, P. Wu, W. Li and S. Liu, In Situ Green Synthesis of Nitrogen-Doped Carbon-Dot-Based Room-Temperature Phosphorescent Materials for Visual Iron Ion Detection, *ACS Sustainable Chem. Eng.*, 2019, **7**(23), 18801–18809.
- 115 Y. Han, M. Li, J. Lai, W. Li, Y. Liu, L. Yin, L. Yang, X. Xue, R. Vajtai, P. M. Ajayan and L. Wang, Rational Design of Oxygen-Enriched Carbon Dots with Efficient Room-Temperature Phosphorescent Properties and High-Tech Security Protection Application, *ACS Sustainable Chem. Eng.*, 2019, **7**(24), 19918–19924.
- 116 M. Xu, X. Wu, Y. Yang, C. Ma, W. Li, H. Yu, Z. Chen, J. Li, K. Zhang and S. Liu, Designing Hybrid Chiral Photonic Films with Circularly Polarized Room-Temperature Phosphorescence, *ACS Nano*, 2020, **14**(9), 11130–11139.
- 117 B. Wang, Z. Sun, J. Yu, G. I. N. Waterhouse, S. Lu and B. Yang, Cross-linking enhanced room-temperature phosphorescence of carbon dots, *SmartMat*, 2022, **3**(2), 337–348.
- 118 Z. Han, P. Li, Y. Deng and H. Li, Reversible and color-variable afterglow luminescence of carbon dots triggered by water for multi-level encryption and decryption, *Chem. Eng. J.*, 2021, **415**, 128999.
- 119 H. Zhang, J. Liu, B. Wang, K. Liu, G. Chen, X. Yu, J. Li and J. Yu, Zeolite-confined carbon dots: tuning thermally activated delayed fluorescence emission via energy transfer, *Mater. Chem. Front.*, 2020, **4**(5), 1404–1410.
- 120 W. Li, W. Zhou, Z. Zhou, H. Zhang, X. Zhang, J. Zhuang, Y. Liu, B. Lei and C. Hu, A Universal Strategy for Activating the Multicolor Room-Temperature Afterglow of Carbon Dots in a Boric Acid Matrix, *Angew. Chem., Int. Ed. Engl.*, 2019, **58**(22), 7278–7283.
- 121 C. Wang, Y. Chen, T. Hu, Y. Chang, G. Ran, M. Wang and Q. Song, Color tunable room temperature phosphorescent carbon dot based nanocomposites obtainable from multiple carbon sources via a molten salt method, *Nanoscale*, 2019, **11**(24), 11967–11974.
- 122 Z. Zhou, E. V. Ushakova, E. Liu, X. Bao, D. Li, D. Zhou, Z. Tan, S. Qu and A. L. Rogach, A co-crystallization induced surface modification strategy with cyanuric acid modulates the bandgap emission of carbon dots, *Nanoscale*, 2020, **12**(20), 10987–10993.
- 123 Z. Xu, X. Sun, P. Ma, Y. Chen, W. Pan and J. Wang, A visible-light-excited afterglow achieved by carbon dots from rhodamine B fixed in boron oxide, *J. Mater. Chem. C*, 2020, **8**(13), 4557–4563.
- 124 C. Wang, Y. Chen, Y. Xu, G. Ran, Y. He and Q. Song, Aggregation-Induced Room-Temperature Phosphorescence Obtained from Water-Dispersible Carbon Dot-Based Composite Materials, *ACS Appl. Mater. Interfaces*, 2020, **12**(9), 10791–10800.
- 125 J. Qu, X. Zhang, S. Zhang, Z. Wang, Y. Yu, H. Ding, Z. Tang, X. Heng, R. Wang and S. Jing, A facile co-crystallization approach to fabricate two-component carbon dot composites showing time-dependent evolutive room temperature phosphorescence colors, *Nanoscale Adv.*, 2021, **3**(17), 5053–5061.
- 126 W. Jiang, L. Liu, Y. Wu, P. Zhang, F. Li, J. Liu, J. Zhao, F. Huo, Q. Zhao and W. Huang, A green-synthesized phosphorescent carbon dot composite for multilevel anti-counterfeiting, *Nanoscale Adv.*, 2021, **3**(15), 4536–4540.
- 127 Y. Zhu, J. Bai, Z. Huang, G. Yuan, L. Zhang, X. Wang and L. Ren, A universal strategy for preparing carbon quantum dot-based composites with blue and green afterglow luminescence, *Mater. Chem. Front.*, 2021, **5**(23), 8161–8170.
- 128 Z. Song, Y. Liu, X. Lin, Z. Zhou, X. Zhang, J. Zhuang, B. Lei and C. Hu, Multiemissive Room-Temperature Phosphorescent Carbon Dots@ZnAl<sub>2</sub>O<sub>4</sub> Composites by



- Inorganic Defect Triplet-State Energy Transfer, *ACS Appl. Mater. Interfaces*, 2021, **13**(29), 34705–34713.
- 129 M. Madhu and W. L. Tseng, NaCl nanocrystal-encapsulated carbon dots as a solution-based sensor for phosphorescent sensing of trace amounts of water in organic solvents, *Anal. Methods*, 2021, **13**(41), 4949–4954.
  - 130 Y. Zheng, Z. Wang, J. Liu, Y. Zhang, L. Gao, C. Wang, X. Zheng, Q. Zhou, Y. Yang, Y. Li, H. Tang, L. Qu, Y. Zhao and C. Yang, Long-Lived Room Temperature Phosphorescence Crystals with Green Light Excitation, *ACS Appl. Mater. Interfaces*, 2022, **14**(13), 15706–15715.
  - 131 K. Jiang, Y. Wang, C. Cai and H. Lin, Conversion of Carbon Dots from Fluorescence to Ultralong Room-Temperature Phosphorescence by Heating for Security Applications, *Adv. Mater.*, 2018, **30**(26), 1800783.
  - 132 C. Zhang, T. Li, Y. Zheng, M. Zhang, M. Liu, Z. Liu, K. Zhang and H. Lin, Modulating Triplet Excited-State Energy in Phosphorescent Carbon Dots for Information Encryption and Anti-Counterfeiting, *ACS Appl. Mater. Interfaces*, 2021, **13**(36), 43241–43246.
  - 133 R. Gui, H. Jin, Z. Wang, F. Zhang, J. Xia, M. Yang, S. Bi and Y. Xia, Room-temperature phosphorescence logic gates developed from nucleic acid functionalized carbon dots and graphene oxide, *Nanoscale*, 2015, **7**(18), 8289–8293.
  - 134 J. Tan, J. Zhang, W. Li, L. Zhang and D. Yue, Synthesis of amphiphilic carbon quantum dots with phosphorescence properties and their multifunctional applications, *J. Mater. Chem. C*, 2016, **4**(42), 10146–10153.
  - 135 T. Yuan, F. Yuan, X. Li, Y. Li, L. Fan and S. Yang, Fluorescence-phosphorescence dual emissive carbon nitride quantum dots show 25% white emission efficiency enabling single-component WLEDs, *Chem. Sci.*, 2019, **10**(42), 9801–9806.
  - 136 K. Jiang, X. Gao, X. Feng, Y. Wang, Z. Li and H. Lin, Carbon Dots with Dual-Emissive, Robust, and Aggregation-Induced Room-Temperature Phosphorescence Characteristics, *Angew. Chem., Int. Ed. Engl.*, 2020, **59**(3), 1263–1269.
  - 137 Y. Zheng, H. Wei, P. Liang, X. Xu, X. Zhang, H. Li, C. Zhang, C. Hu, X. Zhang, B. Lei, W. Y. Wong, Y. Liu and J. Zhuang, Near-Infrared-Excited Multicolor Afterglow in Carbon Dots-Based Room-Temperature Afterglow Materials, *Angew. Chem., Int. Ed. Engl.*, 2021, **60**(41), 22253–22259.
  - 138 Z. Zhou, Z. Song, J. Liu, B. Lei, J. Zhuang, X. Zhang, Y. Liu and C. Hu, Energy Transfer Mediated Enhancement of Room-Temperature Phosphorescence of Carbon Dots Embedded in Matrixes, *Adv. Opt. Mater.*, 2021, **10**(1), 2100704.
  - 139 L. Mo, X. Xu, Z. Liu, H. Liu, B. Lei, J. Zhuang, Z. Guo, Y. Liu and C. Hu, Visible-light excitable thermally activated delayed fluorescence in aqueous solution from F, N-doped carbon dots confined in silica nanoparticles, *Chem. Eng. J.*, 2021, **426**, 130728.
  - 140 P. Liang, Y. Zheng, X. Zhang, H. Wei, X. Xu, X. Yang, H. Lin, C. Hu, X. Zhang, B. Lei, W. Y. Wong, Y. Liu and J. Zhuang, Carbon Dots in Hydroxy Fluorides: Achieving Multicolor Long-Wavelength Room-Temperature Phosphorescence and Excellent Stability via Crystal Confinement, *Nano Lett.*, 2022, **22**(13), 5127–5136.
  - 141 M. Xu, C. Dong, J. Xu, S. u. Rehman, Q. Wang, V. Y. Osipov, K. Jiang, J. Wang and H. Bi, Fluorinated carbon dots/carboxyl methyl cellulose sodium composite with a temperature-sensitive fluorescence/phosphorescence applicable for anti-counterfeiting marking, *Carbon*, 2022, **189**, 459–466.
  - 142 Y. Liu, M. Al-Salihi, Y. Guo, R. Ziniuk, S. Cai, L. Wang, Y. Li, Z. Yang, D. Peng, K. Xi, Z. An, X. Jia, L. Liu, W. Yan and J. Qu, Halogen-doped phosphorescent carbon dots for grayscale patterning, *Light: Sci. Appl.*, 2022, **11**(1), 163.
  - 143 J. Zhu, X. Bai, X. Chen, H. Shao, Y. Zhai, G. Pan, H. Zhang, E. V. Ushakova, Y. Zhang, H. Song and A. L. Rogach, Spectrally Tunable Solid State Fluorescence and Room-Temperature Phosphorescence of Carbon Dots Synthesized via Seeded Growth Method, *Adv. Opt. Mater.*, 2019, **7**(9), 1801599.
  - 144 K. Jiang, S. Hu, Y. Wang, Z. Li and H. Lin, Photo-Stimulated Polychromatic Room Temperature Phosphorescence of Carbon Dots, *Small*, 2020, **16**(31), 2001909.
  - 145 Y. Gao, H. Zhang, S. Shuang and C. Dong, Visible-Light-Excited Ultralong-Lifetime Room Temperature Phosphorescence Based on Nitrogen-Doped Carbon Dots for Double Anticounterfeiting, *Adv. Opt. Mater.*, 2020, **8**(7), 1901557.
  - 146 Y. Wu, X. Fang, J. Shi, W. Yao and W. Wu, Blue-to-green manipulation of carbon dots from fluorescence to ultralong room-temperature phosphorescence for high-level anti-counterfeiting, *Chin. Chem. Lett.*, 2021, **32**(12), 3907–3910.
  - 147 C. Hao, Y. Bai, L. Zhao, Y. Bao, J. Bian, H. Xu, T. Zhou and F. Feng, Durable room-temperature phosphorescence of nitrogen-doped carbon dots-silica composites for Fe<sup>3+</sup> detection and anti-counterfeiting, *Dyes Pigm.*, 2022, **198**, 109955.
  - 148 M. Cheng, L. Cao, H. Guo, W. Dong and L. Li, Green Synthesis of Phosphorescent Carbon Dots for Anticounterfeiting and Information Encryption, *Sensors*, 2022, **22**(8), 2944.
  - 149 Y. Ni, P. Zhou, Q. Jiang, Q. Zhang, X. Huang and Y. Jing, Room-temperature phosphorescence based on chitosan carbon dots for trace water detection in organic solvents and anti-counterfeiting application, *Dyes Pigm.*, 2022, **197**, 109923.
  - 150 H. y. Wang, L. Zhou, H. m. Yu, X. d. Tang, C. Xing, G. Nie, H. Akafzade, S. y. Wang and W. Chen, Exploration of Room-Temperature Phosphorescence and New Mechanism on Carbon Dots in a Polyacrylamide Platform and their Applications for Anti-Counterfeiting and Information Encryption, *Adv. Opt. Mater.*, 2022, **10**(15), 2200678.
  - 151 X. Bao, E. V. Ushakova, E. Liu, Z. Zhou, D. Li, D. Zhou, S. Qu and A. L. Rogach, On-Off switching of the phosphorescence signal in a carbon dot/polyvinyl alcohol composite for multiple data encryption, *Nanoscale*, 2019, **11**(30), 14250–14255.



- 152 H. Qi, H. Zhang, X. Wu, Y. Tang, M. Qian, K. Wang and H. Qi, Matrix-Free and Highly Efficient Room-Temperature Phosphorescence Carbon Dots towards Information Encryption and Decryption, *Chem. - Asian J.*, 2020, **15**(8), 1281–1284.
- 153 Q. Feng, Z. Xie and M. Zheng, Colour-tunable ultralong-lifetime room temperature phosphorescence with external heavy-atom effect in boron-doped carbon dots, *Chem. Eng. J.*, 2021, **420**, 127647.
- 154 S. Wei, H. Li, X. Yin, Q. Yang, A. Chen, R. Li, J. Wang and R. Yang, Revealing graphitic nitrogen participating in p- $\pi$  conjugated domain as emissive center of red carbon dots and applied to red room-temperature phosphorescence, *New J. Chem.*, 2021, **45**(47), 22335–22343.
- 155 X. Teng, X. Sun, W. Pan, Z. Song and J. Wang, Carbon Dots Confined in Silica Nanoparticles for Triplet-to-Singlet Föster Resonance Energy-Transfer-Induced Delayed Fluorescence, *ACS Appl. Nano Mater.*, 2022, **5**(4), 5168–5175.
- 156 T. Li, C. Wu, M. Yang, B. Li, X. Yan, X. Zhu, H. Yu, M. Hu and J. Yang, Long-Lived Color-Tunable Room-Temperature Phosphorescence of Boron-Doped Carbon Dots, *Langmuir*, 2022, **38**(7), 2287–2293.
- 157 Y. Nie, X. Chen, Y. Wang, W. Lai, N. Zheng and W. Weng, Matrix-free nitrogen-doped carbon dots with room temperature phosphorescence for information encryption and temperature detection, *Microchem. J.*, 2022, **175**, 107126.
- 158 X. Bao, E. Liu, X. Yuan, H. Wang, H. Li and S. Qu, Rational preparation of anti-water phosphorescent carbon-dots and flake C<sub>3</sub>N<sub>4</sub> composites through microwave-heating method for multiple data encryption, *J. Lumin.*, 2022, **248**, 118928.
- 159 Q. Li, S. Meng, Y. Li, D. Cheng, H. Gu, Z. Zhao, Z. Tang, J. Tan and S. Qu, Surface ionization-induced tunable dynamic phosphorescence colors from carbon dots on paper for dynamic multimode encryption, *Carbon*, 2022, **195**, 191–198.
- 160 Y. Wu, E. Xue, B. Tian, K. Zheng, J. Liang and W. Wu, Tunable multimodal printable up-/down-conversion nanomaterials for gradient information encryption, *Nanoscale*, 2022, **14**(19), 7137–7145.
- 161 L. Zhang, P. Cui, B. Zhang and F. Gao, Aptamer-based turn-on detection of thrombin in biological fluids based on efficient phosphorescence energy transfer from Mn-doped ZnS quantum dots to carbon nanodots, *Chemistry*, 2013, **19**(28), 9242–9250.
- 162 R. Knoblauch, B. Bui, A. Raza and C. D. Geddes, Heavy carbon nanodots: a new phosphorescent carbon nanostructure, *Phys. Chem. Chem. Phys.*, 2018, **20**(22), 15518–15527.
- 163 N. Xue, J. Yao, C. Shi, X. Wang, W. Shi and C. Lu, Nanosheet-Filled Polymer Film from Flow-Induced Coassembly: Multiscale Structure Visualization and Application, *Langmuir*, 2018, **34**(47), 14204–14214.
- 164 X. Lu, J. Zhang, Y. N. Xie, X. Zhang, X. Jiang, X. Hou and P. Wu, Ratiometric Phosphorescent Probe for Thallium in Serum, Water, and Soil Samples Based on Long-Lived, Spectrally Resolved, Mn-Doped ZnSe Quantum Dots and Carbon Dots, *Anal. Chem.*, 2018, **90**(4), 2939–2945.
- 165 C. Lu, Q. Su and X. Yang, Ultra-long room-temperature phosphorescent carbon dots: pH sensing and dual-channel detection of tetracyclines, *Nanoscale*, 2019, **11**(34), 16036–16042.
- 166 F. Zhao, T. Zhang, Q. Liu and C. Lü, Aphen-derived N-doped white-emitting carbon dots with room temperature phosphorescence for versatile applications, *Sens. Actuators, B*, 2020, **304**, 127344.
- 167 J. Liu, X. Kang, H. Zhang, Y. Liu, C. Wang, X. Gao and Y. Li, Carbon dot-based nanocomposite: Long-lived thermally activated delayed fluorescence for lifetime thermal sensing, *Dyes Pigm.*, 2020, **181**, 108576.
- 168 F. Murru, F. J. Romero, R. Sanchez-Mudarra, F. J. Garcia Ruiz, D. P. Morales, L. F. Capitan-Vallvey and A. Salinas-Castillo, Portable Instrument for Hemoglobin Determination Using Room-Temperature Phosphorescent Carbon Dots, *Nanomaterials*, 2020, **10**(5), 825.
- 169 G. Hu, Y. Xie, X. Xu, B. Lei, J. Zhuang, X. Zhang, H. Zhang, C. Hu, W. Ma and Y. Liu, Room temperature phosphorescence from Si-doped-CD-based composite materials with long lifetimes and high stability, *Opt. Express*, 2020, **28**(13), 19550–19561.
- 170 Q. Su, L. Gan, Y. Zhu and X. Yang, Dual-emissive fluorescence and phosphorescence detection of cholesterol and glucose based on carbon dots-cyanuric acid complex quenched by MnO<sub>2</sub> nanosheets, *Sens. Actuators, B*, 2021, **335**, 129715.
- 171 J. Wang, X. Sun, W. Pan and J. Wang, A fluorescence and phosphorescence dual-signal readout platform based on carbon dots/SiO<sub>2</sub> for multi-channel detections of carbaryl, thiram and chlorpyrifos, *Microchem. J.*, 2022, **178**, 107408.
- 172 M. Fu, Z. Feng, J. Wang, Y. Zhu, L. Gan and X. Yang, Creatine-based carbon dots with room-temperature phosphorescence employed for the dual-channel detection of warfarin, *Appl. Surf. Sci.*, 2022, **571**, 151298.
- 173 Z. Feng, J. Wang, X. Chen, J. Liu, Y. Zhu and X. Yang, Employing metformin-directed carbon dots with room-temperature phosphorescent towards the dual-channel detection of L-tryptophan, *Colloids Surf., B*, 2022, **210**, 112236.
- 174 Y. Tang, C. Huang, H. Tang and M. Guo, Nitrogen-doped carbonized polymer dots activated by alkalinity of arginine for multicolor multi-platform sensor, *Colloids Surf., B*, 2022, **216**, 112517.
- 175 J. Tan, Z. Yi, Y. Ye, X. Ren and Q. Li, Achieving red room temperature afterglow carbon dots in composite matrices through chromophore conjugation degree controlling, *J. Lumin.*, 2020, **223**, 117267.
- 176 Y. Liu, H. Yang, C. Ma, S. Luo, M. Xu, Z. Wu, W. Li and S. Liu, Luminescent Transparent Wood Based on Lignin-Derived Carbon Dots as a Building Material for Dual-Channel, Real-Time, and Visual Detection of Formaldehyde Gas, *ACS Appl. Mater. Interfaces*, 2020, **12**(32), 36628–36638.





- 177 J. Huang, J. Zhu, G. Yang, Y. Zhu, X. Xu and G. Pan, Lifetime-tunable green room temperature phosphorescence of carbon dots by the multi-step modification, *Opt. Express*, 2021, **29**(25), 41014.
- 178 H. Shi, Z. Niu, H. Wang, W. Ye, K. Xi, X. Huang, H. Wang, Y. Liu, H. Lin, H. Shi and Z. An, Endowing matrix-free carbon dots with color-tunable ultralong phosphorescence by self-doping, *Chem. Sci.*, 2022, **13**(15), 4406–4412.
- 179 F. Yan, C. Yi, Z. Hao, Y. Wang, M. Xu, K. Zhou, F. Shi and J. Xu, Solid-state carbon dots with orange phosphorescence and tunable fluorescence via in-situ growth in phthalimide crystal matrix, *Colloids Surf., A*, 2022, **650**, 129626.
- 180 Q. Feng, Z. Xie and M. Zheng, Room temperature phosphorescent carbon dots for latent fingerprints detection and in vivo phosphorescence bioimaging, *Sens. Actuators, B*, 2022, **351**, 130976.
- 181 J. Shi, Y. Zhou, J. Ning, G. Hu, Q. Zhang, Y. Hou and Y. Zhou, Prepared carbon dots from wheat straw for detection of Cu(2+) in cells and zebrafish and room temperature phosphorescent anti-counterfeiting, *Spectrochim. Acta, Part A*, 2022, **281**, 121597.
- 182 C. Xia, S. Tao, S. Zhu, Y. Song, T. Feng, Q. Zeng, J. Liu and B. Yang, Hydrothermal Addition Polymerization for Ultrahigh-Yield Carbonized Polymer Dots with Room Temperature Phosphorescence via Nanocomposite, *Chemistry*, 2018, **24**(44), 11303–11308.
- 183 S. Hu, K. Jiang, Y. Wang, S. Wang, Z. Li and H. Lin, Visible-Light-Excited Room Temperature Phosphorescent Carbon Dots, *Nanomaterials*, 2020, **10**(3), 464.
- 184 Y. Zhu, Z. Feng, Z. Yan and X. Yang, Promoting the transfer of phosphorescence from the solid state to aqueous phase and establishing the universal real-time detection based on the smartphone imaging, *Sens. Actuators, B*, 2022, **371**, 132529.
- 185 J. Zhang, X. Lu, D. Tang, S. Wu, X. Hou, J. Liu and P. Wu, Phosphorescent Carbon Dots for Highly Efficient Oxygen Photosensitization and as Photo-oxidative Nanozymes, *ACS Appl. Mater. Interfaces*, 2018, **10**(47), 40808–40814.
- 186 C. Shi, J. Yao, X. Wang, X. Wen, W. Shi and C. Lu, A triplet state energy transfer material design concept enables enhanced visualization applications, *J. Mater. Chem. C*, 2019, **7**(45), 14170–14180.
- 187 D. C. Green, M. A. Holden, M. A. Levenstein, S. Zhang, B. R. G. Johnson, J. Gala de Pablo, A. Ward, S. W. Botchway and F. C. Meldrum, Controlling the fluorescence and room-temperature phosphorescence behaviour of carbon nanodots with inorganic crystalline nanocomposites, *Nat. Commun.*, 2019, **10**(1), 206.
- 188 X. Sun, J. Zhao, X. Wang, W. Pan, G. Yu and J. Wang, The phosphorescence property of carbon dots presenting as powder, embedded in filter paper and dispersed in solid solution, *J. Lumin.*, 2020, **218**, 116851.
- 189 E. A. Stepanidenko, P. D. Khavlyuk, I. A. Arefina, S. A. Cherevko, Y. Xiong, A. Doring, G. V. Varygin, D. A. Kurdyukov, D. A. Eurov, V. G. Golubev, M. A. Masharin, A. V. Baranov, A. V. Fedorov, E. V. Ushakova and A. L. Rogach, Strongly Luminescent Composites Based on Carbon Dots Embedded in a Nanoporous Silicate Glass, *Nanomaterials*, 2020, **10**(6), 1063.
- 190 W. Miao, W.-S. Zou, Q. Zhao, Y. Wang, X. Chen, S. Wu, Z. Liu and T. Xu, Coupling room-temperature phosphorescence carbon dots onto active layer for highly efficient photodynamic antibacterial chemotherapy and enhanced membrane properties, *J. Membr. Sci.*, 2021, **639**, 119754.
- 191 G. Tang, C. Wang, K. Zhang, Y. Wang and B. Yang, Deep-Blue Room-Temperature Phosphorescent Carbon Dots/Silica Microparticles from a Single Raw Material, *Langmuir*, 2021, **37**(45), 13187–13193.
- 192 Y. Zhai, P. Wang, X. Zhang, S. Liu, J. Li, Z. Chen and S. Li, Carbon dots confined in 3D polymer network: Producing robust room temperature phosphorescence with tunable lifetimes, *Chin. Chem. Lett.*, 2022, **33**(2), 783–787.
- 193 Q. Wu, L. Wang, Y. Yan, S. Li, S. T. Yu, J. G. Wang and L. Huang, Chitosan-Derived Carbon Dots with Room-Temperature Phosphorescence and Energy Storage Enhancement Properties, *ACS Sustainable Chem. Eng.*, 2022, **10**(9), 3027–3036.
- 194 J. V. Rowley, P. A. Wall, H. Yu, M. J. Howard, D. L. Baker, A. Kulak, D. C. Green and P. D. Thornton, Triggered and monitored drug release from bifunctional hybrid nanocomposites, *Polym. Chem.*, 2022, **13**(1), 100–108.
- 195 H. Wang, H. Yu, A. Al-Zubi, X. Zhu, G. Nie, S. Wang and W. Chen, Self-Matrix N-Doped Room Temperature Phosphorescent Carbon Dots Triggered by Visible and Ultraviolet Light Dual Modes, *Nanomaterials*, 2022, **12**(13), 2210.

